FLASH FLOOD RISK ASSESSMENT BASED ON HISTORICAL MEASURED AND SATELLITE DAILY RAINFALL DATA: KYRENIA REGION, NORTHERN CYPRUS

A THESIS SUBMITTED TO THE GRADUATE SCHOOL OF APPLIED SCIENCES OF NEAR EAST UNIVERSITY

By
NOUR ATEF ALIJL

In Partial Fulfilment of the Requirements for The Degree of Master in Science In Civil and Environmental Engineering

NICOSIA, 2020

NOUR ATEF ALIJL

FLASH FLOOD RISK ASSESSMENT BASED ON HISTORICAL MEASURED AND SATELLITE DAILY RAINFALL DATA: KYRENIA REGION, NORTHERN CYPRUS

NEU 2020

FLASH FLOOD RISK ASSESSMENT BASED ON HISTORICAL MEASURED AND SATELLITE DAILY RAINFALL DATA: KYRENIA REGION, NORTHERN CYPRUS

A THESIS SUBMITTED TO THE GRADUATE SCHOOL OF APPLIED SCIENCES
OF
NEAR EAST UNIVERSITY

By
NOUR ATEF ALIJL

In Partial Fulfilment of the Requirements for
The Degree of Master in Science
In
Civil and Environmental Engineering

NICOSIA, 2020

Nour Atef ALIJL: FLASH FLOOD RISK ASSESSMENT BASED ON HISTORICAL MEASURED AND SATELLITE DAILY RAINFALL DATA: KYRENIA REGION, NORTHERN CYPRUS

Approval of Director of Graduate School of Applied Sciences

Prof. Dr. Nadire ÇAVUŞ

We certify this thesis is satisfactory for the award of the degree of Masters of Science in Civil and Environmental Engineering

Examining Committee in Charge:

Prof. Dr. Hüseyin Gökçekuş	Committee Chairman, Supervisor, Den of Civil and Environmental Engineering, Department of Civil Engineering, NEU
Assist. Prof. Dr. Youssef KASSEM	Co-Supervisor, Department of Mechanical Engineering, NEU
Assoc. Prof. Dr. Fidan Aslanova	Department of Civil and Environmental Engineering, NEU
Assoc. Prof. Dr. Hüseyin ÇAMUR	Department of Mechanical Engineering, NEU
Assist.Prof. Dr. Anoosheh Iravnian	Department of Civil and Environmental Engineering, NEU

I hereby declare that all information in this document has been obtained and presented in accordance with academic rules and ethical conduct. I also declare that, as required by these rules and conduct, I have fully cited and referenced all material and results that are not original to this work.

Name, last name: Nour Atef Alijl
Signature: Nour alijl
Date:24-07-2020

ACKNOWLEDGEMENTS

I express my sincere gratitude to those who have made it possible for me to conclude this study.

I really want to express my sincere appreciation to my supervisors, who made this study achievable. Special thanks go to my supervisor Prof. Dr. Hüseyin Gökçekuş and co-supervisor Assist. Prof. Dr. Youssef Kassem for their guideline, support, and assistance.

I wish to acknowledge my great parents, family, and friends: Atef; my father, Heyam; my mother, Hiba, Najwa, and the rest of my sisters and brothers, Hedaya, Taleb, Mohammed, and Nafn; my friends. Who shared me the hard time and supported me to overcome all challenges have been through.

The study carried out through a world pandemic COVID-19. So, this hard work is acknowledged primarily for the soul of people who suffered from disaster as well as those suffering from flash flood in my country, Kyrenia and the rest of the world.

To my Family…

ABSTRACT

The aim of this study is to develop a flash-floods risk mitigation plan, which appears to be very beneficial for municipalities, provincial administrators, authorities to reduce the impact of the flash flood in the Kyrenia region, Northern Cyprus. In this work, rainfall data were collected from nearest station for period (1995-2016) for the Kyrenia to be used for distrubtion and retuern period analysis ,to define the policies regarding water resource management, which is a source of data for flood hazard mitigation. Furthermore, flood inundation and hazard maps were defined by utilizing SAGA, QGIS, ArcGIS, 2D HEC RAS, and HEC -HMS software then determine the degree of risk and to identify strategies based on quantitative risk analysis by developing risk matrix. Moreover, five factors thematic maps, namely; land use; elevation; slope; flow accumulation, peak discharge, which affect flood events, were classified using spatial analysis tool in ArcGIS software to generate flood hazard maps. Peak discharge and excess of precipitation were computed by rainfall-runoff simulation by applying the Synthetic unit hydrograph (SUH)method using HEC-HMS. Excess of precipitation was used as input for hydraulic 2D flood modeling using HEC-RAS based on unsteady flow analysis for selected design periods 5,25,50,100 and 200 years. As final results, catastrophic risk areas are distributed in significant downstream. Also, lowlands are most vulnerable to flood occurrence while the low and minor risk area at the highest land, such as five mountains. Based on that risk matrix was developed to determine degrees of risk then to define strategies.

İn conclusion, proposed flash flood mitigation plan includes strategies to reduce flood losses human life and constructed structures across Kyrenia, proposed hazard and inundation risk maps to assess planners and decision-makers for the potential impact of floods to avoid.in addition of developed web platform data and information to be shared globally and locally.

Keywords: Flash Flood, Hazard map, Inundation map, Risk matrix, DEM,
Rainfall distribution, HEC-RAS, Mitigation plan, Strategies .

ÖZET

Bu çalışmanın amacı, Kuzey Kıbrıs'ın Girne bölgesinde flaş selinin etkisini azaltmak için belediyeler, il yöneticileri ve yetkililer için çok faydalı görünen bir sel baskını riskini azaltma planı geliştirmektir. Bu çalışmada, taşkın tehlikesinin azaltılması için bir veri kaynağı olan su kaynakları yönetimi ile ilgili politikaları tanımlamak amacıyla Girne'nin dağıtım ve geri kazanım dönemi analizinde kullanılması için en yakın istasyondan (1995-2016) yağış verileri toplanmıştır. . Ayrıca, taşkın su baskını ve tehlike haritaları, SAGA, QGIS, ArcGIS, 2D HEC RAS ve HEC-HMS yazılımları kullanılarak tanımlanmış, daha sonra risk derecesini belirlemek ve risk matrisi geliştirerek nicel risk analizine dayalı stratejileri belirlemek. Ayrıca, beş faktör tematik harita; arazi kullanımı; yükseklik; eğim; taşkın olaylarını etkileyen akış birikimi, pik deşarjı, taşkın tehlike haritaları oluşturmak için ArcGIS yazılımında mekansal analiz aracı kullanılarak sınıflandırılmıştır. Tepe deşarjı ve fazla yağış, HEC-HMS kullanılarak Sentetik birim hidrograf (SUH) yöntemi uygulanarak yağış-akış simülasyonu ile hesaplanmıştır. Yağış fazlası, seçilen tasarım periyotları 5,25,50,100 ve 200 yıl için kararsız akış analizine dayanan HEC-RAS kullanılarak hidrolik 2D taşkın modellemesi için girdi olarak kullanılmıştır. Nihai sonuçlar olarak, yıkıcı risk alanları önemli aşağı yönde dağılmıştır. Ayrıca, alçak araziler sel oluşumuna karşı en savunmasızken, beş dağ gibi en yüksek arazideki düşük ve küçük riskli alanlar. Bu risk temelinde, risk derecelerini belirlemek ve sonra stratejileri tanımlamak için geliştirilmiştir. Sonuç olarak, önerilen sel baskını azaltma planı, Girne genelinde sel kayıplarını ve yaşam yapılarını azaltmak için stratejiler, planlamacıları ve karar vericileri önlemek için sellerin potansiyel etkisi açısından değerlendirmek için önerilen tehlike ve su baskını risk haritalarını içermektedir. küresel olarak ve yerel olarak paylaşılacak veri ve bilgiler.

Anahtar Kelimeler: Ani Taşkın, Tehlike haritası, su baskın haritası, risk matrisi, DAM, yağış dağılımı, HEC-RAS, etki azaltma planı, stratejiler.

TABLE OF CONTENTS

LIST OF TABLES

LIST OF FIGURES

LIST OF ABBREVATIONS

2D HEC RAS:	2D Hydrologic Engineering Center's - River Analysis System
A:	Area
A-D:	Anderson-Darling
AIGA:	American Institute of Graphic Arts
ArcGIS:	ARC Geographic Information System
CGRS:	Cyprus Geodetic Reference System 1993
CN:	Curve Number
C-s:	Chi-squared
CV:	Coefficient of Variation
DEM:	Digital Elevation Model
DS:	Down stream
E:	Elevation
EPSG 6312:	Cyprus Local Transverse Mercator
F:	Flow accumulation
FR:	Factors Rates
FWS:	Flood Warning Systems
GFA:	Geomorphic Flood Area
HEC HMS:	Hydrologic Engineering Center - Hydrologic Modeling System
HEC-Geo-HMS:	The Geospatial Hydrologic Modeling Extension
HU:	unit hydrograph
IDF:	Intensity Duration Frequency

IDW:	Inverse distance weighting
K:	Kurtosis
K-S:	Kolmogorov-Smirnov
L:	Land use
L:	length of stream
Max:	Maximum
MCM:	The Mathematical Contest in Modeling
Min:	Minimum
NDVI:	Normalized Difference Vegetation Index
NMHSs:	National Meteorological and Hydrological Services
NRCS:	Natural Resources Conservation Service
NWP:	Numerical Weather Prediction
OS-Geo:	Open Source Geospatial Foundation
P:	Peak discharge
QGIS:	Quantum Geographic Information System
R:	Daily Rainfall
RL:	Risk Levels
S:	Slope
S:	Skewness
SA:	Saudi Arabia
SAGA:	System for Automated Geoscientific Analyses
SCS:	Soil Conservation Services
SCS-CN:	Soil Conservation Services - Curve Number

SD:	Standard Deviation
SMA:	Soil Moisture Accounting
SRTM:	Shuttle Radar Topographic Mission
SUH:	Synthetic unit hydrograph
Tc:	Time of Concentration
Tlag:	lag Time
TWİ:	Topographic Wetness Index
US:	Upper stream
WSE:	Water Surface Elevations

CHAPTER 1
INTRODUCTION

1.1 Background

Flash floods are natural hazards frequently occurred over the world and a harmful risk for human beings, and flood impact is about 30% of the economic losses mete out to natural hazards (Natural,2005). Moreover, 175,000 people were killed in a total 1816 flood worldwide in 1975–2001(Jonkman,2005) Moreover, around 2.3 billion people from the third of the world's population has been affected by floods in last 20 years due to climate changes which have been estimated by the United Nations (Human,2015).

Conducting and planning for the flood risk which is identified as 'hazard' (Associated,1970) can be translated into maps developed by computer modeling showing the boundary of the terrain at risk as well as flow depth, water surface elevations(WSE) and velocities to inform the public, planners, decision-maker about prone areas inflicted by the flood.

1.2 Problem Statement

Kyrenia had inflicted by negative impacts from flooding due to heavy and torrential rainfall in its urban environment. No official Figures are announced on the extent of urban flood damage. Many flash floods were reported by news and social media, as summarised .

The heavy rainfall in Girne (Kyrenia) and Lefkosa (Nicosia) as reported by relief web news on February 27, 2010. Which affected more than 3000 people without any reported cases for death and injury, around 700 homes,56 office,s, and 27 vehicles were informed to damage. The response towards floods was providing food packages and blanket to victims by north Cyprus Red Crescent Society.

The heavy rain in Kyrenia, as reported by the Cyprus scene on January 18, 2014, led to flooding in many houses and workplaces, which built-in river beds, the response towards flood was to build an embankment around the main river.

The heavy rain, as reported by LGC news on November 3, 2017, has caused severe flooding, causing traffic chaos, the response towards floods was advising people to avoid using roads until the water subsides.

Torrential rainfall, as reported by LGC news on November 3, 2017, has caused a flash flood causing damage road network in the Cypriot capital Nicosia and the partial closure of a motorway linking the city to Kyrenia, a historic harbor town on the northern coast. also of four people were killed when their car was swept away during heavy rain as shown in Figure 1.1 .

Figure 1.1: Divers search for a swollen river in Kyrenia, North Cyprus, on December 6, 2018.

The heavy rain and thunderstorms, as reported by LG news on January 8, 2020, caused a flood in Kyrenia, which affected shops, businesses, and homes also of Guzelyurt reservoir are overflowing as shown in Figure 1.2 .

Figure 1.2: Guzelyurt reservoir was overflowing, LG NEWS January 8, 2020

1.3 Study Objectives

The study aims at developing a flash-floods risk mitigation plan which appears to be very beneficial for municipalities, provincial administrators, authorities to reduce the impact of a flash flood, the sub-objectives include the following:

- Define the policies regarding water resource management, which is a source of data for flood hazard mitigation. This can be achieved by estimating and analyzing the frequency of rainfall.
- Generate flood inundation & hazard maps using SAGA, QGIS, ArcGIS and 2D HEC RAS, and HEC HMS software.
- Determine the degree of risk and identify strategies based on quantitative risk analysis by developing a risk matrix.
- Identify possible communal and structural strategies to be considered by authorities, planners, decision-makers, and stakeholders.

1.4 Thesis Outline

The presented study will extend knowledge of flash flood risk assessment and added new values for integration between local community local authorities, municipalities planner, and decision making to mitigate flash flood. Also, an Updated approach was proposed using the latest technology, updated spatial planning, and updated web platform data to be shared with all stakeholders. The operating procedures are illustrated in Figure 1.3 ; the preceding chapters provide an updated approach starting from the literature review, data analysis then define strategies as summarised .

- Chapter 1 presents a brief description of the study objective, the reasons for selecting Kyrenia .
- Chapter 2 presents a literature review and theory explanations.
- Chapter 3 presents the proposed methodology to conclude this study.
- Chapter 4 presents achieved results and discuss analysis then to recommend a proposed mitigation plan which includes analysis, define risk matrix and identified strategies

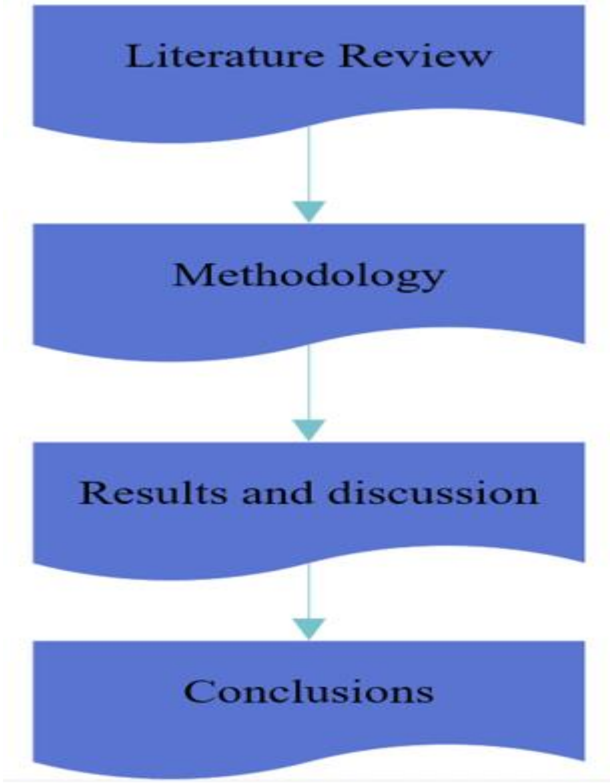

Figure 1.3: Thesis outline

CHAPTER 2
LITERATURE REVIEW

2.1 Background

Flood risksFlood risks, which have increased in recent years due to changing physical characteristics of the hydrological system caused by climate changed all over the world In this decade. Flood losses are high occurred in this time as a consequence of rapid development by encroachment on flood-prone areas, environmental degradation, climate changed, and failure to manage the flood risk by the competent governmental and engineering bodies. Water resources are the main component of natural systems that might be affected by climate change that caused floods and droughts.

Flash flood prevention has become a global issue, representing a significant challenge, as the recent time to forecast floods is limited. Flash flood events are still not predicted in their entirety, spatially and temporally, even by more sophisticated alert systems, due to the incapacity of current methods to identify the location and time of smallscale intense rainfall (Sun et al. 2012).

Flash floods can be prevented by applying structural methods such as physical constructions, and non-structural methods, such as those using knowledge and experience to reduce the impact of risks, particularly by policies and laws, public awareness, training, and education (Sun et al. 2012).

A well-coordinated and balanced combination of both structural and non-structural measures are recommended as a long-term flood mitigation strategy (Faisal et al. 1999). Still, in the last decade, the non-structural ones have acquired a significant role (NCAR 2010), mainly because the structural methods are costly and do not provide 100% protection against floods (Faisal et al. 1999).

These non-structural measures are explained as any measures that do not involve physical constructions, using knowledge and practice to reduce risks and impacts, mainly through policies and laws, public awareness, training, and education (Sun et al., .2012).

In many countries, they introduced flood warning systems (FWS) to reduce the impact of flood risk by warning people in flood-prone areas to evacuate and protect their property. The behavior of individuals, businesses, and government entities before, during, and immediately after a disaster can dramatically affect the impact and recovery time.Previous studies over the world were conducted to assess flood risk are summarized :

- The study proposed a flood risk map in Awlad Toq-Sharq, Southeast Sohag, Egypt by applying total runoff estimate and multi-criteria analysis for various factors such as elevation; slope, drainage network, lithology, topographic wetness index (TWİ) and land use using spatial tool analysis in GIS (Abu El-Magd,2020).
- The study proposed a risk flood matrix technique applied in Taibah and Islamic universities catchment in Saudi Arabia (SA). Developed matrix based on the probability of flood occurrence and inundation flood map generated by HEC-RAS software. A quantitative analysis was conducted to assess flood economic losses impact (Elfeki,2019).
- The study proposed a new flash flood warning scheme for Yuncheng, Shanxi in China by analysis impact of critical hazard index, the impact of rainfall duration, and impact of antecedent rainfall using spatial analysis tool in GIS (Huang,2019).
- The study proposed an integrated model using KINEROS2 and HEC-RAS software to forecast flash flood occurrence in Northern Vietnam, which is a massive flash flooding prone area—using different precipitation datasets which conclude a relation between flow velocity, water level and streamflow power to predict flood occurrence on the gauged data (Nguye,2019).
- The study aims to evaluate factors that affect flood magnitude and to provide aspatial and temporal variation of flood inundated areas in the Zambezi basin in Zimbabwean by simulating rainfall using HEC-HMS and flood routing using HEC-RAS (Nharo,2019).
- The study aims to generate a Flash flood inundations map for the Hadahe River basin in northeastern China by analyzing future extreme rainfall analysis and generate flood hydrograph based on gauge data, climate model, and digital elevation model(DEM) using HEC-HMS software (Zhang,2019).

- The study is conducted in Northern Cyprus which ıncludes Kyrenia Mountains and the Karpass Peninsula to analysis rainfall using L-moments with time series clustering approaches to identify homogeneous regions using dynamic data , The accuracy of the estimated quantiles was evaluated through Monte Carlo simulations (Zaifoglu,2018).
- The study is conducted in Kyrenia region to analysis sustainable urban growth which has effect on enviromental or economic issue using spatial layers such as slopes, soil prdouctivity, roads distrances and environmental protection zones using GIS tools ro generate map to show areas at risk to reduce impact of disasters.(Kara,2018).
- The study proposed a geomorphic flood area (GFA) tool using digital elevation models and Quantum QGIS software; the proposed mechanism has numerous applications in flood risk assessment and hazards over vast areas. It may be used by geomorphological and hydrological communities which aim to develop a web platform for global flood mapping (Samela,2018).
- The study is conducted in the United States, including Iowa -Cedar River watershed and Alabama - Black Warrior River to compare two new generated hydrodynamic model for flow inundation maps using 2D HEC-RAS, and low-complexity tools HAND(AutoRoute and Height Above the Nearest Drainage), which result in as fast predictions tool in large-scale hyper-resolution operational frameworks (Afshari,2018).
- The study proposed a flood map for Ksour Mountains in south Algeria by simulating rainfall and runoff using HEC-HMS software after analysis intensity duration frequency (IDF), time series, catchment area, and meteorological data (Derdour,2018).
- The study proposed a scheme integration of hydrological models based on runoff simulation and rainfall data mutually with FIM to assess the flash flood risk impact for Wadi Fatimah in the arid region in Saudi Arabia (SA) Using GIS techniques. This concludes the integrated scheme is a useful tool to evaluate the impact of flood risk and hazard also the dam construction with limited measured hydrological data (Elfeki,2017).
- The study proposed a flash hazard map that helps in water harvesting and catchment management in wadi Qena in Egypt based on the analysis of rainfall and morphometric parameters using GIS tools(Taha,2017).
- The study aims to generate a flash flood risk map in the Nuweiba area, Egypt, based on field analysis, rainfall modeling for the ungauged area by applying the SCS method

considering land cover and soil properties also morphometric analysis of drainage basins using GIS and ARC-hydro software (Abuzied,2016).

- The study aims to define flood-prone areas in watersheds in Turkey by extracting a hydrological model considering the wetness index using QGIS and SAGA software by using the Digital Elevation Model (DEM) of the study area. Also of the analyzed hydraulic model using HEC-RAS under a wide range of return period-flood events to generate flood inundation maps. That results in taking safety measures against flood impact on human beings and economic losses in urban areas, particularly (Aksoy,2016).
- The proposed study aims to generate a flood depth map for Starozubersky based on my many factors which affect flood event such as land use; water level; precipitation and elevation by applying runoff simulation using SCS method and compute curve number(CN) using HEC-HMS, HEC-RAS AND ARCGIS for catchment area analysis (Divin,2016).
- The study aims to generate flood risk maps in Crete in Greece by calibrating and weight all factors which affect flood events such as flow accumulation, slopes, elevation, land use, rainfall intensity, and geology by applying different scenarios using GIS software (Kourgialas,2016).
- The study was conducted in Najran City, Kingdom of Saudi Arabia (KSA) to extract a flood hazard map based on many factors such as runoff, soil influences; surface slope; surface roughness, drainage density, and distance to the main channel and land cover by estimate weighted scores, simulate rainfall using HEC-HMS and hydrological analysis using HEC-Geo-HMS and Arc-hydro (Elkhrachy,2015).

2.2 Flash Flood Definition:

Flash Flood is sudden water covering of land surface not usually covered by water as a result of localized high rainfall intensity. It takes place in a time duration that is span counted in minutes, or only a few hours from the event that causes it to happen (excessive rainfall, failure of hydraulic infrastructure, etc.). During a flash flood, there is a sudden rise in the water level in rivers and streams, and flow velocity can be very high. The force of the water can be so great as to tear away boulders, uproot trees, and destroy bridges and buildings that stand in its path.

2.3 Frequency of Rainfall Analysis

Generally, rainfall is an essential input to rainfall-runoff modeling. In hydrological design applications, design rainfall (intensity–duration–frequency) data is used to obtain rainfall intensity at a given region for a given duration (Kundwa,2019). The intensity duration frequency data are widely used in the planning and designing of stormwater infrastructure and flood management works (Tfwala,2019). In deriving intensity duration frequency curves, one of the primary steps is fitting an appropriate probability distribution to at-site rainfall data. The selection of a probability distribution that gives the best fit to the observed rainfall or flood data is an important research topic in the field of statistical hydrology (Okoli,2019). No theoretical distribution can be considered that it can exclusively characterize the annual rainfall profile (Michaelides,2009).

Thus, the analysis of rainfall/precipitation data mainly depends on its distribution type. Many researchers have studied the precipitation (rainfall) characteristics using different distribution functions in different parts of the world. Thus, Table 2.1 summarizes the previous scientific studies that have been conducted across the globe on the selection of probability distributions in rainfall/flood frequency analyses.

Table 2.1:Summary of previous applications of probability distributions in rainfall/flood analysis

Reference	Data used	Best fit distribution	Country
(Phien.1984)	Annual maximum rainfall data (durations of 1 h to 31 days)	Log-Pearson type 3	Thailand, India, Laos, and the USA

Table 2.1:Continued

Reference	Data used	Best fit distribution	Country
(Tortorelli,1999)	15, 30, and 60 min and 1, 2, 3, 6, 12, and 24 h and 1, 3, and 7 days of rainfall	Generalized logistic	Oklahoma, USA
(Şen,1999)	Monthly total rainfall data	Gamma	Libya
(Ogunlela,2001)	Daily and monthly annual maximum rainfall data	Log-Pearson type 3	Nigeria
(Zalina,2002)	Annual maximum rainfall data (1-h duration)	Generalized Extreme value	Malaysia
(Tao,2002)	Annual maximum rainfall series (5 min and 1-h duration)	Generalized Extreme value	Southern Quebec, Canada
(Lee,2005)	Annual maximum rainfall data (24-h duration)	Log-Pearson type 3	Taiwan
(Phien.1984)	Annual maximum rainfall data (durations of 1 h to 31 days)	Log-Pearson type 3	Thailand, India, Laos, and the USA
(Şen,1999)	Monthly total rainfall data	Gamma	Libya

Table 2.1:Continued

Reference	Data used	Best fit distribution	Country
(Ogunlela,2001)	Daily and monthly annual maximum rainfall data	Log-Pearson type 3	Nigeria
(Zalina,2002)	Annual maximum rainfall data (1-h duration)	Generalized Extreme value	Malaysia
(Tao,2002)	Annual maximum rainfall series (5 min and 1-h duration)	Generalized Extreme value	Southern Quebec, Canada
(Lee,2005)	Annual maximum rainfall data (24-h duration)	Log-Pearson type 3	Taiwan
(Y.,2007)	Annual maximum rainfall data (1-h duration)	Mixed-exponential	Malaysia
(Kwaku,2007)	Annual maximum rainfall series (1-, 2-, 3-, 4- and 5-day durations)	Log-normal	Ghana
(Hanson,2008)	Daily rainfall	3-parameter Pearson-III distribution and 4-parameter Kappa distribution	Unite State

Table 2.1: Continued

Reference	Data used	Best fit distribution	Country
(Sharma,2008)	Annual rainfall	Gamma	Cyprus
(Johnson,2007)	Annual maximum rainfall series (24-h duration)	Log-normal	Pantnagar, India
(Green,2012)	5-min to 72-h durations	Generalized Extreme value	Australia
(Khudri,2013)	1–12 h, 1–7 days rainfall	Generalized Extreme value	Australia
(Mamoon,2014)	Annual maximum rainfall	Generalized extreme value and four parameters generalized gamma	Bangladesh
(Montaseri,2014)	Annual maximum rainfall 24-h duration	Pearson type 3	Qatar
(Mandal,2014)	Monthly and annual rainfall data	Pearson type 3	Northwest of Iran
(Subyani,2015)	Annual, seasonal and monthly maximum daily rainfall	Normal for annual, post-monsoon, and summer seasons. Lognormal, Weibull, and Pearson 5 for pre-monsoon, monsoon, and winter seasons, respectively.	Sagar Island

Table 2.1: Continued

Reference	Data used	Best fit distribution	Country
(Hassan,2015)	24-h annual maximum rainfall data	Extreme value type 1 and Log-Pearson type 3	Al-Madinah City, Saudi Arabia
(Mamoon, 2016)	24-h annual maximum rainfall data	Extreme value type 1 and Log-Pearson type 3	Al-Madinah City, Saudi Arabia
(Amin,2016)	6h rainfall	Generalized Pareto, Wake-by and Generalized Extreme value	Peninsular Malaysia
(Mohamed, 2016)	Annual maximum rainfall series (average of 36 years)	Generalized Extreme value	Qatar
(Agbonaye,2017)	24h annual maximum rainfall	Log-Pearson type 3	Northern regions of Pakistan
(Yuan,2018)	Annual rainfall	Normal and Gamma distribution	Sudan
(Alam,2018)	Annual maximum series of daily rainfall data	Generalized Extreme value	Southeastern Nigeria
(Alam,2018)	Annual maximum hourly rainfall	Log-Pearson type 3	Japan
(Meena,2019)	Extreme values for precipitation	Gaussian/normal	Bangladesh

Table 2.1: Continued

Reference	Data used	Best fit distribution	Country
(Baghel,2019)	Maximum monthly rainfall	Pearson type 3 and Log-Pearson type 3	Bangladesh
(Parchure,2019)	Daily rainfall	Gamma	Cooch Behar

2.4 Runoff Effects on The Flood Event

To understand fundamentals of floods it is necessary to comprehend the basics of the hydrologic cycle that covers "the cyclic movement of water from the sea to the atmosphere by evaporation, and then by precipitation back to the earth where it runs to the sea through streams or through groundwater flow" as shown in Figure 2.1 hypothetically (Usul 1994, 1).

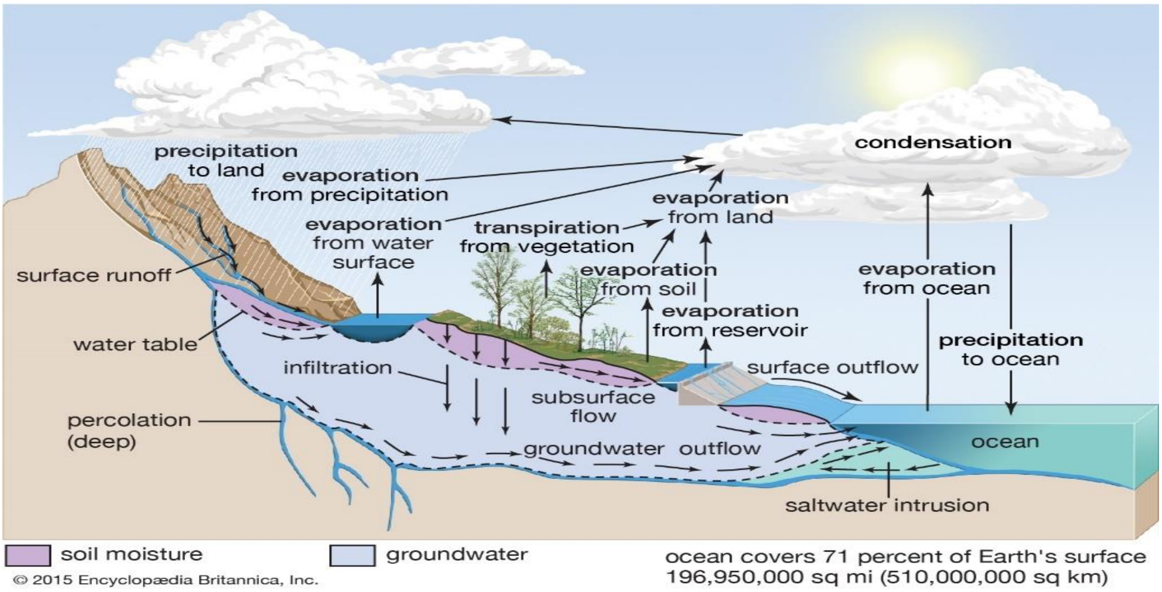

Figure 2.1: The Hydrologic Cycle.

Hydrological cycle elements such as precipitation, streamflow, evaporation, and infiltration are essential to investigate while dealing with flood hazards within a specific period in a given area, as per (Merz 2004) flood hazard is generally defined as the probability of the occurrence of potentially damaging flood events.

Prone areas inflicted by flood hazards are generally determined by the previous flooding occurrences and morphology by the hydrological and hydraulic analysis (FEMA 2003). The establishment of systematic patterns for the runoff is possible, which influences flood events. The depth and intensity of precipitation, river discharge, snow depth and density, lake level, infiltration rate, groundwater Table 2. level, water quality, evaporation rates, etc. It can be empirically measured for a specified period. Flood intensity depends on vast variables which include physical terrain features, or past and present hydro-meteorological rainfall data. Merz (2004) as summarized :

- Inundation depth based on discharges from a flood frequency curve.
- Flow velocity (geomorphology).
- Duration of the flood, which influenced by the rate of soil infiltration and drainage capacity).
- Rainfall intensity affects the water rate to rise.

2.5 Flood Hazard and Inundation Maps

Flood hazard and inundation maps define the boundary of the prone area at particular risk, as shown in Figure 2.2, which creates a basis f to reduce the impact of flood risk reduction programs and subsequent actions. Also, it provides the spatial distribution of the flood risk can be shared globally and locally. Maps convey information for many applications in flood defense and disaster management" (Merz 2004, 1). Moreover, it shows the intensity of flood situations and associated exceedance probability.

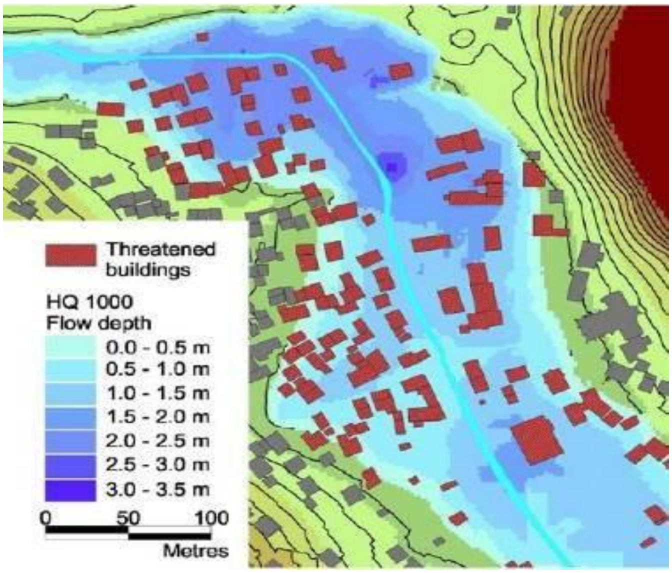

Figure 2.2: Flood inundation map (Merz,2004)

Through latest released of geographic information systems software's such as QGIS, Arc GIS, and HEC-RAS, the inundation and hazard maps can be generated in real-time and associated of hydrological forecast system and land use plan for a particular area (Pilon 2003, 28), which help in define mitigation plans, policies, and guidelines based on the zone risk as shown in Figure 2.3 .

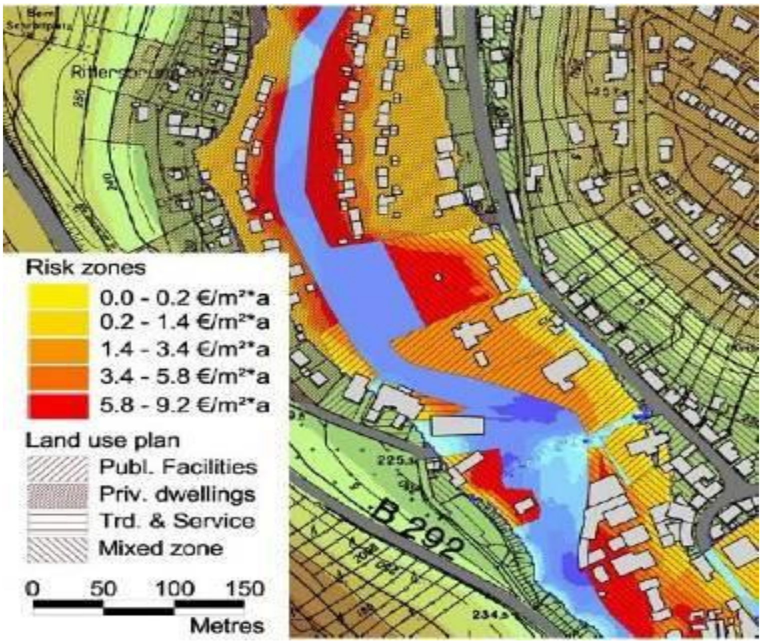

Figure 2.3: Flood Hazard map associated with land use (Merz,2004)

2.6 Hydraulic - Hydrologic Modeling and Software Support

Due to massive development in advanced computational technology today, a vast number of spatial tools are available to technical experts, to define and explain flood mitigation plans and program to decision-makers, public and local authorities about real-time forecasts and early warnings by updating the information, and providing visual and quantitative results regarding the state of conditions.

Geographic Information Systems (GIS) that provide a computer-based information and manipulation system are combined with hydraulic models that are supplied by computerized programs summarized in Table 2.2 . However, before the generation of flood inundation maps, a high resolution of digital elevation model (DEM) which can be downloaded using USGS earth explorer.

Input and analyzed information from a variety of sources can be combined as a series of layers, provided that the data can be identified in terms of the common denominator of the specific location" (Pilon 2003, 30). For example, to estimate infiltration rates for forecasting purposes, information on vegetation cover can be combined with information on the land slope and soil type.

Table 2.2: Geographic Information Systems software's

	Software	Aim
QGIS	QGIS is an open-source, user-friendly system Geographic Information System (GIS) licensed under the general public license (GPL), which is an official project of the Geospatial Foundation (OSGeo).	Catchment area analysis and flow delineation. Flow accumulation, direction, and channel networks.

Table 2.2: Continued

	Software	Aim
ArcGIS	ArcGIS is a geographic information system utilized to working with maps and geographic information maintained by the Environmental Systems Research Institute	Spatial analysis tools for: Raster maps classifications. Overlay weighted maps
HEC-HMS	The Hydrologic Modeling System (HEC-HMS) is designed to simulate the complete hydrologic processes of dendritic watershed systems.	Runoff simulation and modeling
HEC-RAS	Hydrologic Engineering Center's -River Analysis System	2D modeling for flood mapping

2.7 Flood Protection and Flood Risk Mitigation

The most widely used flood protection method through history is the construction of the parallel embankment on streams banks or sea to avoid the highest flood water level. Nevertheless, structural measures are widely used and experienced to avoid settlements caused by floods, such as the levees (embankments), channel, dikes, dams,etc…, which considered as a temporary solution creating more destructive flood disasters during future events.

Many cases were reported throughout the world. For example, the Mississippi River Flood in 1993, was a milestone in the US for abandoning the policy, which is wholly based on investing in flood-control structures as Cigler states (1996, 192). According to Cigler (1996, 193), "containing water in a narrow and high channel to protect farms and urban areas, on the other hand, has the opposite effect." The intervention based on direct physical actions, which include the construction of levees and river reclamations, causes significant destructive impacts on floodplains due to an increase in the speed of water flow and high water surface elevation at the same time. "In essence, the river adjusts in response to human tampering with the floodplain, and these adjustments induce humans to make constant and costly upgrades in structures" as claimed by Cigler (1996, 193).

In context, the proposed structural measures approach for flood management is temporary to solve problems and mitigate flood risk. However, it leads to even more severe impacts in the long-term. It's proved in so many cases that the structural interventions to protect life and property from high floodwaters cannot always be safe enough.

Therefore, Integration between local communal strategies and structural measures is required, which includes interventions based on mechanisms of rules to influence human behavior indirectly. The traditional engineering approach of flood risk management, which considers material point, which is significant for decision-makers' interventions. For these interventions, a collective term is non-structural measures. These non-structural options, based upon the realistic understanding that floods are imminent, to keep people away from increasing of water surface elevation due to floods. The policy includes regulations and guideline related to land use, zoning acquisition, relocation of permanent property; also of using proof material for buildings, raising awareness by learning and education, financial aspects such as flood insurance, utilizing new technology by using flood warning systems, disaster preparedness and response planning). In conclusion, this approach is an attempt to reduce the flood hazard, which affects human life and their property, with a commitment to long-term risk management of all factors that affect flood risk. The management system is required to have targeted objectives, accountable, monitored, and flexible response towards newly updated circumstances and new information (Cigler 1996, 193).

"Despite the apparent need for a more balanced approach toward floodplain 'management' through a wise combination of structural and non-structural options, flood 'control' (just applying fundamental techniques) has been the dominant philosophy" (Cigler 1996, 193). Hence the main question rose by Cigler (1996, 193) is how a 'balanced' approach should be achieved by societies as shown in Figure 2.4 reservoirs, dams, etc., the term called 'structural measures' is commonly
used in the literature.

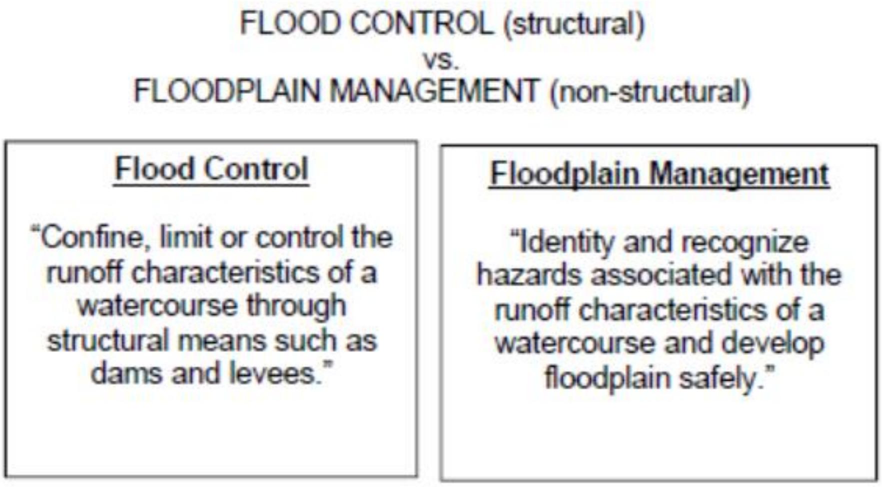

Figure 2.4: Structural and non-structural strategies (FEMA,2003)

After explaining the mentioned strategies above to reduce the flood risk, residual risks should be considered and shared within involved stakeholders, by applying effective insurance system, aids, donations, cross-financing, and extra taxes to reduce risk impact. Also, the full utilization and re-distribution of resources are required, which include financial management services and experts qualified in public relations, commercial, public administration, and insurance.

Urban planning for prone areas inflicted by flood, the combination of the selected choices, should be determined according to possible scenarios that "can be understood as conceptualized futures for the flood risk system" (Schanze 2006).

2.7 Risk Characteristics

Studying risk perception by applying a standrd approach, which is defined as the development of a taxonomy for hazards to understand the nature of the risk and human response towards these risks. An often-used approach is a psychometric paradigm (Slovic, 1987). They were using this paradigm individuals rate judgments about risk characteristics, as described above, on an ordinal scale. Alternatively, the characterizations of voluntariness, dread, the knowledge of those exposed, and the degree of control over the flood risk are used. For natural hazards, dread is often characterized as worry. Understanding of the Risk among those who are exposed is defined as awareness and control over the risk as preparedness (Slovic et al. 1984).The mentioned characteristics will be explained in the subsections of this chapter summarized below.

2.7.1 Awareness

Flood risk awareness explained by consciousness or knowledge of the risk which is exposed to stakeholders, including individuals and groups. Levels of awareness could be summarized as per the following:

1. Expert awareness which can be achieved by risk assessments based probabilities.
2. Underestimation of the Probability of hazard occurrence or consequences that can be determined by experts.
3. The exposed stakeholders are ignorant of their risk.

The defined policy is responsible for raising risk awareness. Flood risk awareness increases when (1) society is confronted with a hazard; and (2) information and education about the danger is more widely available, and this information has implications for appropriate corrective actions (King 2000). However, local communities tend to eliminate associated risks with non-occasional events; in results, awareness may be declined (Arthurton 1998). The first example is the flood inundation of the Maas River in the Netherlands during 1925 and 1993, with 70 years reduced awareness among local affected communities. Residents around river banks were not prepared for inundation in 1993. The subsequent event with similar severity was only two years later in 1995. The local communities were much better prepared since the memory of the 1993 event was still present in their minds. The provision of education of the public and information increases awareness typically. The second example, the improvement of environmental observation in the European Union, increased data availability to analyze flood risk data by experts (Mitchell 2003).

2.7.2 Preparedness

The capability of handling a flood is an explanation of preparedness based on proposed strategies and recovery plans during the inundation period (van der Veen and Logtmeijer 2005; Floodsite 2006)s. Preparedness can be outlined and explained in many aspects, including social, technical, institution, and economical. The technological part related to technical measures applied to individuals or groups on an or group basis to reduce the impact of the flood on the material which informed to be damaged. Proposed permanent measures, which include changing exterior and interior materials of future designed buildings, temporary reinforcement, and emergency equipment. The social aspects refer to corrective actions taken by individuals before and during a flood event as well as handling the flood consequences related to personal skills, knowledge, and awareness towards flood events. Local administrators and authorities should have emergency supplies; proper evacuation also plans,volunteers. In the long-term restrictive work schedules of employees limit the recruitment of volunteers.for example, if local employees cannot get an exemption from work for emergency response situations. To prevent significant post-flood inconvenience and social distress, residents, as well as businesses, have to be prepared for the post-flood phase, and community relationships have to be strengthened (Buckland and Rahman 1999). The institutional dimension refers to the design and communication of an action plan in case of flooding (e.g., evacuation schemes and training of emergency staff). The economic dimension refers to the reduction of the financial risk of potential victims of a flood utilizing insurance. Similarly, insurance with well-structured premiums can stimulate the introduction of measures aimed at the reduction of damages and losses (Kron 2002).

CHAPTER 3
METHODOLOGY

3.1 Description

In this study, Figure 3.1 shows the proposed methodology to develop flood risk mitigation plan in Kyrneia region, Northern Cyprus. It consists of the analysis of catchment area and flow delineation , land use and soil characteristic using three softwares. The rainfall data are gathered from available nearest station and satellite data for period 1995 to 2016 . Runoff simulation is conducted using hydrological modelling system software to calculate peak discharge and excess of precipitation for different design periods ranges from 5 to 200 years. Also, hydrological river analysis software is employed to determine and generate inundation flood depths map.Hazard flood map is extracted by applying spatial tool analysis using ArcGIS, for five different thematic maps. A risk flood matrix is generated to estimate probability and impact of flood hazards based on pervious study (Moser1997; Elfeki et al. 2017). Quantitative risk analysis to be conducted in future works, define strategies for local communities and structure.

The proposed method requires the main set of input data as summarized .

- Extracted a Digital Elevation Model (DEM) in Geo-Tiff format
- Rainfall data.
- Extracted land use and soil characteristic using landsat-8 bands.

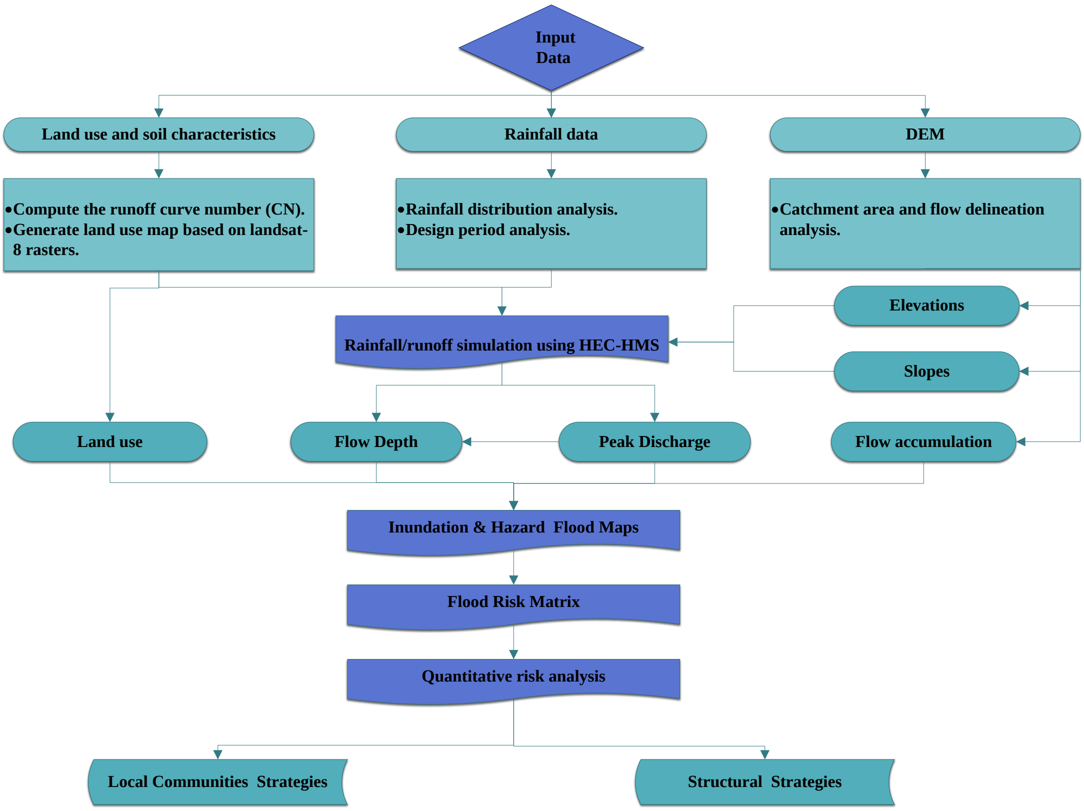

Figure 3.1: schematic description for proposed methodology (own elaboration)

3.2 Extracted A Digital Elevation Model (DEM)

Digital elevation data are 3D models of the earth's surface, usually stored as a pixel grid (Raster) format where each cell has the average elevation value of its coverage area. The primary source of free global elevation data is from the Shuttle Radar Topographic Mission (SRTM).Digital elevation model (DEM) was extracted using USGS earth explorer https://earthexplorer.usgs.gov/, to be used as input in QGIS hydrlogical model analysis which includes flow direction, flow accumulation, slopes, channel networks and subbasins.

3.3 Hydrologic Modelling Using QGIS and SAGA Plug.

Quantum GIS (QGIS) is an open source product .as such as the software is constantly developing and being improved by the world wide GIS community (QGIS,2015). QGIS 3.12.1 version was used for hydrological modeling in addition of using SAGA plug which has some powerful terrain and hydrological analysis tool (SAGA,2017). In order to generate a hydrological flow model, digital elevation model (DEM) should be free of 'sinks' or depressions points that will capture water flow by applying algorithm Wang Liu method , By applying basic terrain analysis tool , terrain parameter in shape file format will be created which include the following as shown in Figures 3. 2 and 3.3 .

- A grid of slope.
- Wetness index to produces a grid showing water accumulation.
- Channels in a vector file of drainage channels. One of the attributes of this data is the Strahler order which is a measure of the order of the stream in the drainage network.
- Drainage Basins in shape file of water catchments.

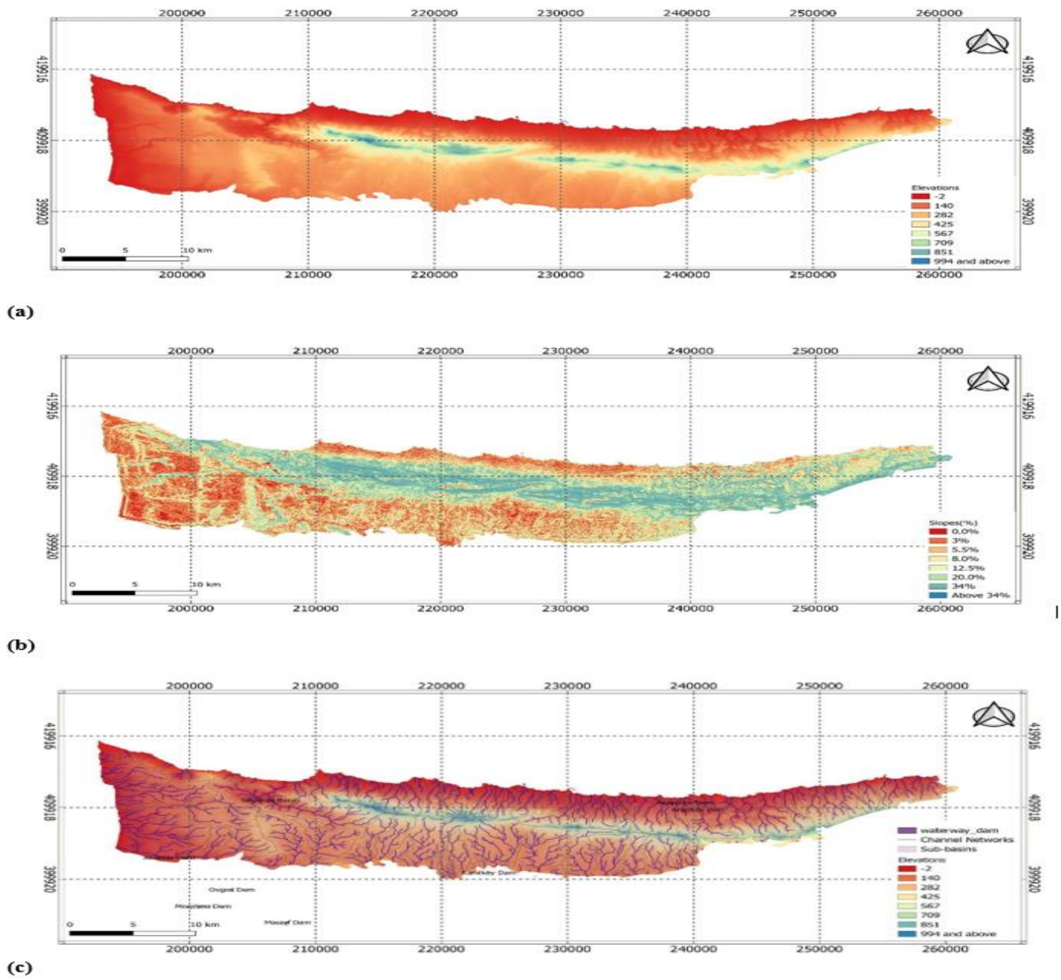

Figure 3.2: Extracted elevation(a), slopes(b), channel networks and subbasins(c) using QGIS and SAGA plug

3.4 Wang Liu Method

SAGA plug for filling sinks using three different algorithms argument methods: Planchon and Darboux (2001); wang.liu.2006 and xxl.wang.liu.2006. Based on previous studies Wang liu. 2006 method was employed to identify and fill surface depressions in DEMs. The method was enhanced to allow the creation of hydrologically sound elevation models, i.e. not only to fill the depressions but also to preserve a downward slope along the flow path. If desired, this is accomplished by preserving a minimum slope gradient (and thus elevation difference) between cells. In contrast, employed method directly computes a spill elevation value for each grid cell without prior delineation of the catchments of depressions. This is due to the use of the least-cost search algorithm, which enables to progressively build the optimal flow paths and propagate spill elevation values from outlets to interior grid cells. With one pass of processing, our method is able to produce the depression-less DEM and identify the locations and depth of the surface depressions. The least-cost search is also known as the best-first search or priority-first search in the field of artificial intelligence and computer science (Cormen et al. 1996, Sedgewick 2002). The general philosophy of the algorithm is to give first priority to the direction with the least-cost for further search and expansion (Dechter and Pearl 1988). The cost in the search is defined as the spill elevation. Boundary cells of the DEM are regarded as the potential outlets. Their original elevation values are assigned as their spill elevations, which represent the costs for seeding the optimal paths.

$$h(bk) = S(bk) = E(bk) \qquad (3.1)$$

where h(bk) is the estimate of cost for boundary cell bk to be the outlet for optimal path search, S(bk) is the spill elevation of boundary cell bk, and E(bk) is the original elevation value of boundary cell bk.

Among these candidate outlets, the highest priority is given to the cell with the least-cost (the lowest elevation). It serves as the root of the first tree for optimal path search and expansion. The least-cost boundary cell is examined as the central cell, and its immediate interior neighbors are identified. Links between these neighboring interior cells and the central cell are added as the first generation of edges for the tree. The links represent the optimal paths for these interior cells because connecting these interior cells to the lowest outlet will lead to the lowest possible spill elevations for these interior cells. The interior neighbors of the lowest cell on the border of the DEM are added as the nodes of the tree, and the least-cost boundary cell is then marked as a processed node. We employ the following function to estimate the costs for optimal path expansion from these neighbors:

$$h(nj) = S(nj) = maxf\{E(nj\ ), S(c)g\}, j \sim 1, 2, \ldots, 7 \qquad (3.2)$$

where nj is the jth neighbor of the central cell c, h(nj) is the estimate of the cost for expanding optimal paths from the neighbor cell nj, S(nj) is the spill elevation value for neighbor cell nj, E(nj) is the original elevation of the jth neighbor of the central cell c, and S(c) is the spill elevation of the central cell c, which represents the cost of the optimal path established so far between the root and the central cell being processed. As water may not flow back toward the previous downstream cell, there are seven possible neighbors for an interior cell to expand the optimal paths. As shown in equation (2), the spill elevation value for the neighbor cell nj is estimated based on its original elevation E(nj) and spill elevation S(c) of the central cell, and is assigned as the cost for expanding the optimal path from this neighbor cell.

3.5 Rainfall Data

Daily rainfall data were collected from Meteorological department located in North Nicosia and satellite data for design period from 1995 to 2016. In order to define the policies regarding water resource management which is a source of data for flood hazard mitigation, this can be achieved by estimating and analyzing frequency of rainfall by selecting 37 distribution function models are utilized in order to determine the best-fit probability distributions by applying three goodness-of-fit tests (Kolmogorov–Smirnov, Anderson–Darling, and Chi-squared) using easy fit software. Moreover, six formulas are employed to forecast the return period in years of maximum daily rainfall in the selected region.

3.6 Probability Distributions

The choice of the probability distribution models is essential to select the best-fit probability distribution for a specific location. In this section, nominated distribution models were summarized in Table 3.1 to analyze the characteristic of daily rainfall in Kyrenia region in Northern Cyprus. The method of maximum-likelihood is utilized to estimate the parameters of distribution models.

Table 3.1: Probability density and cumulative distribution of used distribution functions

Distribution function	Probability Density Function	Cumulative Distribution Function
Beta	$f(R) = \frac{1}{B(\alpha_1,\alpha_2)} \frac{(R-a)^{\alpha_1-1}(b-R)^{\alpha_2-1}}{(b-a)^{\alpha_1+\alpha_2-1}}$	$F(R) = I_z(\alpha_1,\alpha_2)$
Four-Parameter Burr	$f(R) = \frac{\alpha k\left(\frac{R-\gamma}{\beta}\right)^{\alpha-1}}{\beta\left(1+\left(\frac{R-\gamma}{\beta}\right)^{\alpha}\right)^{k+1}}$	$F(R) = 1-\left(1+\left(\frac{R-\gamma}{\beta}\right)^{\alpha}\right)^{-k}$
Three-Parameter Burr	$f(R) = \frac{\alpha k\left(\frac{R}{\beta}\right)^{\alpha-1}}{\beta\left(1+\left(\frac{R}{\beta}\right)^{\alpha}\right)^{k+1}}$	$F(R) = 1-\left(1+\left(\frac{R}{\beta}\right)^{\alpha}\right)^{-k}$
Cauchy	$f(R) = \left(\pi\sigma\left(1+\left(\frac{R-\mu}{\sigma}\right)^{2}\right)\right)^{-1}$	$F(R) = \frac{1}{\pi} arctan\left(\frac{R-\mu}{\sigma}\right) + 0.5$
Four-Parameter Dagum	$f(R) = \frac{\alpha k\left(\frac{R-\gamma}{\beta}\right)^{\alpha k-1}}{\beta\left(1+\left(\frac{R-\gamma}{\beta}\right)^{\alpha}\right)^{k+1}}$	$F(R) = 1-\left(1+\left(\frac{R-\gamma}{\beta}\right)^{-\alpha}\right)^{-k}$
Three-Parameter Dagum	$f(R) = \frac{\alpha k\left(\frac{R}{\beta}\right)^{\alpha k-1}}{\beta\left(1+\left(\frac{R}{\beta}\right)^{\alpha}\right)^{k+1}}$	$F(R) = 1-\left(1+\left(\frac{R}{\beta}\right)^{-\alpha}\right)^{-k}$

Table 3.1: Continued

Distribution function	Probability Density Function	Cumulative Distribution Function
Three-Parameter Erlang	$f(R) = \dfrac{(R-\gamma)^{m-1}}{\beta^m \Gamma(m)} exp\left(-\dfrac{R-\gamma}{\beta}\right)$	$F(R) = \dfrac{\Gamma_{(R-\gamma)/\beta}(m)}{\Gamma(m)}$
Two-Parameter Erlang	$f(R) = \dfrac{(R-\gamma)^{m-1}}{\beta^m \Gamma(m)} exp\left(-\dfrac{R}{\beta}\right)$	$F(R) = \dfrac{\Gamma_{(R)/\beta}(m)}{\Gamma(m)}$
Two-Parameter Exponential	$f(R) = \lambda\, exp\big(-\lambda(R-\gamma)\big)$	$F(R) = 1 -\ exp\big(-\lambda(R-\gamma)\big)$
One-Parameter Exponential	$f(R) = \lambda\, exp(-\lambda R)$	$F(R) = 1 -\ exp(-\lambda R)$
Three-Parameter Gamma	$f(R) = \dfrac{(R-\gamma)^{\alpha-1}}{\beta^\alpha \Gamma(\alpha)} exp\left(-\left(\dfrac{R-\gamma}{\beta}\right)\right)$	$F(R) = \dfrac{\Gamma_{(R-\gamma)/\beta}(\alpha)}{\Gamma(\alpha)}$
Two-Parameter Gamma	$f(R) = \dfrac{R^{\alpha-1}}{\beta^\alpha \Gamma(\alpha)} exp\left(-\left(\dfrac{R}{\beta}\right)\right)$	$F(R) = \dfrac{\Gamma_{R/\beta}(\alpha)}{\Gamma(\alpha)}$
Generalized Extreme Value	$f(R) = \begin{cases} \dfrac{1}{\sigma} exp\Big(-\Big(1 + k\dfrac{R-\mu}{\sigma}\Big)^{-1/k}\Big)\Big(1 \\ \dfrac{1}{\sigma} exp\Big(-\dfrac{R-\mu}{\sigma} - exp\Big(-\dfrac{R-\mu}{\sigma} \end{cases}$	$F(R) = \begin{cases} exp\Big(-\Big(1 + k\dfrac{R-\mu}{\sigma}\Big)^{-1/k} \\ exp\left(-exp\left(-\dfrac{R-\mu}{\sigma}\right)\right) \end{cases}$

Table 3.1: Continued

Distribution function	**Probability Density Function**	**Cumulative Distribution Function**
Four-Parameter Generalized Gamma	$f(R) = \frac{k(R-\gamma)^{k\alpha-1}}{\beta^{k\alpha}\Gamma(\alpha)} xp\left(-\left(\frac{R-\gamma}{\beta}\right)^{k}\right)$	$F(R) = \frac{\Gamma_{((R-\gamma)/\beta)^k}(\alpha)}{\Gamma(\alpha)}$
Three-Parameter Generalized Gamma	$f(R) = \frac{k(R)^{k\alpha-1}}{\beta^{k\alpha}\Gamma(\alpha)} xp\left(-\left(\frac{R}{\beta}\right)^{k}\right)$	$F(R) = \frac{\Gamma_{((R)/\beta)^k}(\alpha)}{\Gamma(\alpha)}$
Generalized Logistic	$f(R) = \begin{cases} \frac{\left(1+k\frac{R-\mu}{\sigma}\right)^{-1-1/k}}{\sigma\left(\left(1+k\frac{R-\mu}{\sigma}\right)^{-1/k}\right)^{2}} & k \neq 0 \\ \frac{\exp\left(-\frac{R-\mu}{\sigma}\right)}{\sigma\left(1+\exp\left(-\frac{R-\mu}{\sigma}\right)\right)^{2}} & k = \end{cases}$	$F(R) = \begin{cases} \frac{1}{\left(1+k\frac{R-\mu}{\sigma}\right)^{-1/k}} & k \neq 0 \\ \frac{1}{1+\exp\left(-\frac{R-\mu}{\sigma}\right)} & k = 0 \end{cases}$
Generalized Pareto	$f(R) = \begin{cases} \frac{1}{\sigma}\left(-\left(1+k\frac{R-\mu}{\sigma}\right)^{-1-1/k}\right) & k \neq \\ \frac{1}{\sigma} exp\left(-\frac{R-\mu}{\sigma}\right) & k = \end{cases}$	$F(R) = \begin{cases} 1-\left(1+k\frac{R-\mu}{\sigma}\right)^{-1-1/k} & k \\ 1-exp\left(-\frac{R-\mu}{\sigma}\right) & k \end{cases}$
Maximum Extreme Value Type 1	$f(R) = \frac{1}{\sigma} exp\left(-\frac{R-\mu}{\sigma} - exp\left(-\frac{R-\mu}{\sigma}\right)\right)$	$F(R) = exp\left(-exp\left(-\frac{R-\mu}{\sigma}\right)\right)$

Table 3.1: Continued

Distribution function	Probability Density Function	Cumulative Distribution Function
Minimum Extreme Value Type 1	$f(R) = \frac{1}{\sigma} exp\left(\frac{R-\mu}{\sigma} - exp\left(-\frac{R-\mu}{\sigma}\right)\right)$	$F(R) = 1 - exp\left(-exp\left(-\frac{R-\mu}{\sigma}\right)\right)$
Three-Parameter Inverse Gaussian	$f(R) = \sqrt{\frac{\lambda}{2\pi(R-\gamma)}} exp\left(-\frac{\lambda(R-\gamma-\mu)^2}{2\mu^2(R-\gamma)}\right)$	$F(R) = \Phi\left(\sqrt{\frac{\lambda}{R-\gamma}}\left(\frac{R-\gamma}{\mu} - 1\right)\right) + \Phi\left(-\sqrt{\frac{\lambda}{R-\gamma}}\left(\frac{R-\gamma}{\mu} + 1\right)\right) exp\left(\frac{2\lambda}{\mu}\right)$
Log-Gamma	$f(R) = \frac{\left(ln(R)\right)^{\alpha-1}}{R\beta^{\alpha}\Gamma(\alpha)} exp\left(\frac{-ln(R)}{\beta}\right)$	$F(R) = \frac{\Gamma_{(ln(R)/\beta)^k}(\alpha)}{\Gamma(\alpha)}$
Logistic	$f(R) = \frac{exp\left(-\frac{R-\mu}{\sigma}\right)}{\sigma\left\{1 + exp\left(-\frac{R-\mu}{\sigma}\right)\right\}^2}$	$F(R) = \frac{1}{1 + exp(-R)}$
Log-Logistic	$f(R) = \left(\left(\frac{\beta}{\alpha}\left(\frac{R}{\alpha}\right)^{\beta-1}\right) \Big/ \left(1 + \frac{R}{\alpha}\right)^{\beta}\right)^2$	$F(R) = \frac{1}{\left(1 + \frac{R}{\alpha}\right)^{-\beta}}$

Table 3.1: Continued

Distribution function	**Probability Density Function**	**Cumulative Distribution Function**
Two-Parameter Inverse Gaussian	$f(R) = \sqrt{\frac{\lambda}{2\pi(R-\gamma)}} exp\left(-\frac{\lambda(R-\mu)^2}{2\mu^2 R}\right)$	$F(R) = \Phi\left(\sqrt{\frac{\lambda}{R-\gamma}}\left(\frac{R}{\mu}-1\right)\right) + \Phi\left(-\sqrt{\frac{\lambda}{R-\gamma}}\left(\frac{R}{\mu} + 1\right)\right) exp\left(\frac{2\lambda}{\mu}\right)$
Three-Parameter Lognormal	$f(R) = \frac{1}{(R-\gamma)\sigma\sqrt{2\pi}} exp\left[-\frac{1}{2}\left(\frac{ln(R-\gamma)}{\sigma}\right.\right.$	$F(R) = \Phi\left[\frac{ln(R-\gamma)-\mu}{\sigma}\right]$
Two-Parameter Lognormal	$f(R) = \frac{1}{R\sigma\sqrt{2\pi}} exp\left[-\frac{1}{2}\left(\frac{ln(R)-\mu}{\sigma}\right)^2\right]$	$F(R) = \frac{1}{2} + erf\left[\frac{ln(R)-\mu}{\sigma\sqrt{2}}\right]$
Log-Pearson 3	$f(R) = \frac{1}{R\lvert\beta\rvert\Gamma(\alpha)}\left(\frac{ln(R)-\gamma}{\beta}\right)^{\alpha-1} exp\left(-\right.$	$F(R) = \frac{\Gamma_{(ln(R)-\gamma)/\beta}(\alpha)}{\Gamma(\alpha)}$
Nakagami	$f(R) = \frac{2m^m}{\Gamma(m)\Omega^{\mathrm{m}}} R^{2m-1} e^{\left(-\frac{m}{\Omega}G^2\right)}$	$F(R) = \frac{\gamma\left(m, \frac{m}{\Omega}R^2\right)}{\Gamma(m)}$
Normal	$f(R) = \frac{1}{\sqrt{2\pi\sigma^2}} exp\left(-\frac{R-\mu}{2\sigma^2}\right)$	$F(R) = \frac{1}{2}\left[1 + erf\left(\frac{R-\mu}{\sigma\sqrt{2}}\right)\right]$
Two-Parameter Rayleigh	$f(R) = \frac{R-\gamma}{\sigma^2} exp\left(-\frac{1}{2}\left(\frac{R-\gamma}{\sigma}\right)^2\right)$	$F(R) = 1 - exp\left(-\frac{1}{2}\left(\frac{R-\gamma}{\sigma}\right)^2\right)$

Table 3.1: Continued

Distribution function	Probability Density Function	Cumulative Distribution Function
One-Parameter Rayleigh	$f(R) = \frac{R}{\sigma^2} exp\left(-\frac{1}{2}\left(\frac{R}{\sigma}\right)^2\right)$	$F(R) = 1 - exp\left(-\frac{1}{2}\left(\frac{R}{\sigma}\right)^2\right)$
Wakeby	$R(F) = \xi + \frac{\alpha}{\beta}\left(1 - (1-F)^{\beta}\right) - \frac{\gamma}{\delta}\left(1 - (1-F)^{\delta}\right)$	
Three-Parameter Weibull	$f(R) = \left(\frac{\alpha}{\beta}\right)\left(\frac{R-\gamma}{\beta}\right)^{\alpha-1} exp\left(-\left(\frac{R-\gamma}{\beta}\right)^{\alpha}\right)$	$F(R) = 1 - exp\left(-\left(\frac{R-\gamma}{\beta}\right)^{\alpha}\right)$
Two-Parameter Weibull	$f(R) = \left(\frac{\alpha}{\beta}\right)\left(\frac{R}{\beta}\right)^{\alpha-1} exp\left(-\left(\frac{R}{\beta}\right)^{\alpha}\right)$	$F(R) = 1 - exp\left(-\left(\frac{R}{\beta}\right)^{\alpha}\right)$

3.7 Goodness-of-Fit Test

Validity check for the specified probability distribution model, Goodness-of-fit test statistics are utilized. Kolmogorov-Smirnov (K-S) test, the Anderson-Darling (A-D) test, and Chi-squared (C-s) test are the most well-known empirical distribution function tests (Baghel,2019).

Kolmogorov-Smirnov (K-S) test

$$D = \max_{1 \le i \le n}\left(F(x_i) - \frac{i-1}{n}, \frac{i}{n} - F(x_i)\right) \qquad (3.3)$$

where

$$F_n(x) = \frac{1}{n} \times (Number\ of\ observation \le x) \qquad (3.4)$$

Anderson-Darling (A-D) test

$$A^2 = -n - \frac{1}{n}\sum_{i=1}^{n}(2i-1) \times \left[lnF_X(x_i) + ln\left(1 - F_X(x_{n-i+1})\right)\right] \quad (3.5)$$

where

$F_X(x_i)$ is the cumulative distribution function of the proposed distribution at x_i, for i = 1, 2, . . . , n.

Chi-squared (C-s) test

$$\mathcal{X}^2 = \sum_{i=1}^{k}\frac{(O_i - E_i)^2}{E_i} \quad (3.6)$$

where O_i is the observed frequency for the bin I, and E_i is the expected frequency for the bin I calculated by

$$E_i = F(x_2) - F(x_1) \quad (3.7)$$

where F is the cumulative distribution function of the probability distribution being tested, and x_1, x_2 are the limits for bin i.

3.8 Return Period Analysis

Estimation of the return period (sometimes called the recurrence interval) is one of the essential objectives of the frequency analysis. It is an estimation of the likelihood of an event such as extreme rainfall to occur over an extended period. Return period is a measure of the probable time interval between the occurrence of a given event and that of an equal or more significant event. If the variable (X) equal to or higher than x occurs on the average once in T years, then the probability of occurrence $P(X \geq x)$ of such a variable is shown in the equation.

$$P = \frac{1}{T}(X \geq x) \quad or \quad T = \frac{1}{P}(X \geq x) \quad (3.8)$$

To determine the plotting position, which refers to the probability value assigned to each piece of data to be plotted, several methods have been proposed. Equation (7) is the most plotting position formula which represented.

$$P = \frac{1}{T} = \frac{m-b}{n+1-2b} \qquad (3.9)$$

Where m is the rank of a value in a list ordered by descending magnitude, n is the total number of values to be plotted, b is a parameter, which is different in different formulas ($b = 0.5$ for Hazen; $b = 0.3$ for Chegodayev; $b = 0$ for Weibull; $b = 3/88$ for Blom; $b = 1/3$ for Tukey; and b = 0.44 for Gringoten).

3.9 Assessment of Land Use, Soil Characteristic, and Curve Number (CN).

Surface runoff is defined as the rainfall excess after subtracting the initial, and additional abstractions result from evaporation and infiltration, respectively. Both the infiltration and the potential maximum retention are based on the physical properties of the soil and land surface features of the basin. Physical properties of the soil include textures, compactions, structures, and soil moistures, while surface features include land use, land cover, and topographic characteristics. Consequently, flash flood amounts depend upon rainfall, soil characteristics, land use, land cover, and relief.

The curve number (C.N.) is a mathematical value of the hydrological element which describes the potentiality of the flash flood of the hydrographic basin. The C.N. is influenced by the physical properties of the soil, land use, land cover, and soil moisture aspects. So, the C.N. is considered as a hydrological parameter that expresses the combination of hydrological soil groups and land use, as shown in Table 3.2.Based upon the Natural Resources Conservation Service NRCS, soils are classified into four groups as summarized in Table 3.3 . The NRCS soil group can be identified at the site using either soil properties or the country soil maps.

Table 3.2: Selected land use classes and NRCS curve number (NRCS,2007)

Land use	**Runoff curve numbers by hydrological soil groups**			
	A	**B**	**C**	**D**
Arid -semi-arid				
Herbaceous	-	71	81	89
Oak -aspen	-	48	57	63
Pinyon-juniper	-	58	73	80

Table 3.2: Continued

Land use	**Runoff curve numbers by hydrological soil groups**			
	A	**B**	**C**	**D**
Rural				
Fallow	76	85	90	93
Row crop (contoured	65	75	82	86
small grain	63	75	83	87
pasture	49	69	79	84
close seeded legumes	64	75	83	85
Meadow	30	58	71	78
woods	43	65	76	82
Impervious surface (paved)	98	98	98	98
Urban				
Residential housing	46	65	77	82
Commercial and business	89	92	94	95
Industrial	81	88	91	93
streets and roads	98	98	98	98
Open areas	49	69	79	84
connected impervious areas	98	98	98	98

Table 3.3: Soil classifications (NRCS,2007)

Soil type	Texture
A	Deep sands, deep loess, and silt
B	Shallow loess and sandy loam
C	Clay loam, shallow sandy loam, soils of low organic
D	Clay and salty soils

In this study, Extracted land-use using updated Landsat-8 images dated on 20 February 2020 downloaded from earth explorer, the virtual map was generated using QGIS as shown in Figure 3.3 .

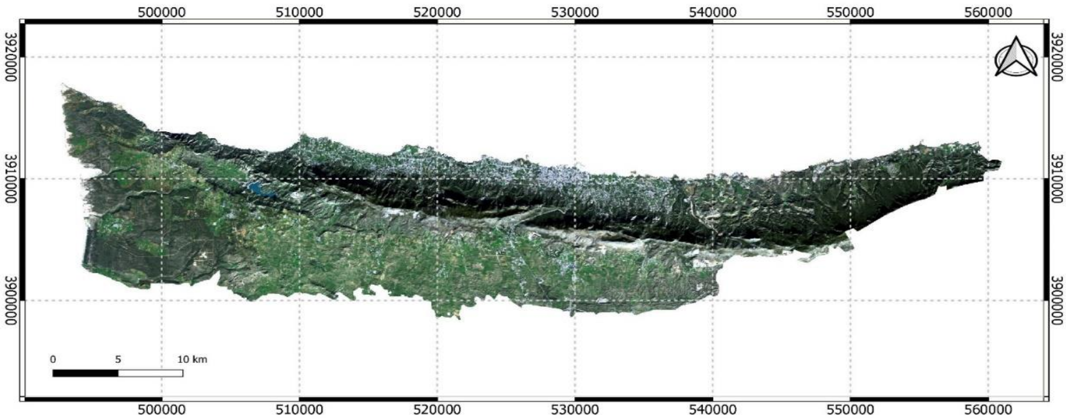

Figure 3.3: Updated Landsat-8 -Kyreina /QGIS

3.10 Rainfall-Runoff simulation model

Runoff simulation consists of four main components, which include basin model, defined metrological data, control specifications, and time-series data using HEC-HMS, which designed to solve many problems related to flow prediction, spillway design and flood impact for various geographic areas [SCHARFFENBERG, FLEMING 2016]. Based on previous studies, the selected methods to calculate the hydraulic loss rate is SCS curve number (C.N.), and for runoff, the rate is the SCS unit hydrograph (H.U.).56 sub-basins extracted using QGIS will be included in the simulation as shown in Figure 3.4.

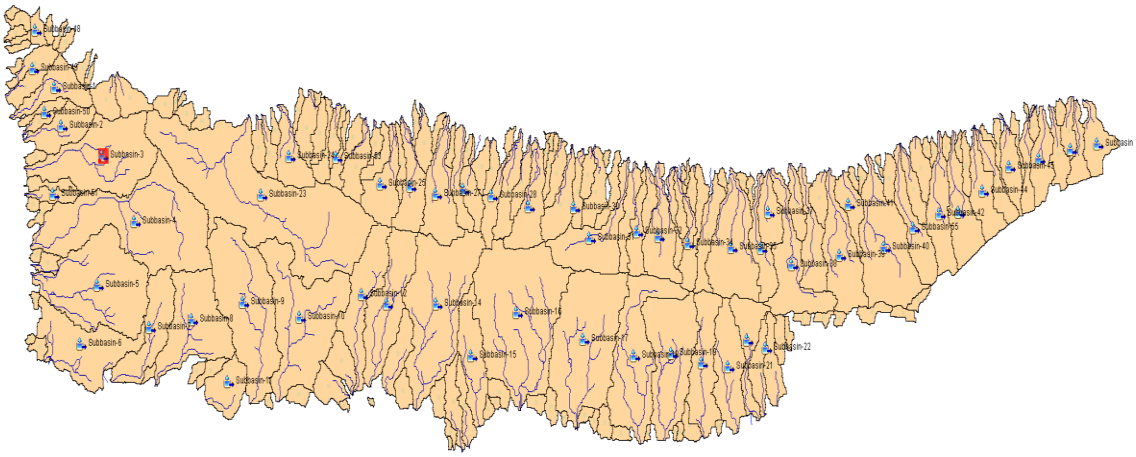

Figure 3.4: Channel network and sub-basins-HEC-HMS

3.10.1. Loss Method

An assortment of different methods is available to simulate infiltration losses (deficit and constant, exponential, Green and Ampt, initial and constant, SCS curve number, Smith Parlange, and Soil Moisture Accounting– SMA).SCS curve number (C.N.) loss method is used to determine the hydrologic loss rate. The Soil Conservation Services (SCS) of the USA (lately renamed as Natural Resources Conservation Services, NRCS) issued a mathematical formula for calculating runoff of hydrographic basin and named SCS Runoff C.N. scheme as follows:

$$Q = \frac{(P - 0.2S)^2}{P + 0.8S} \qquad (3.10)$$

where Q represents the surface runoff amount, P represents the rainfall amount, while S represents the potential maximum retention amount. The potential maximum retention is estimated through the hydrological element named curve number (C.N.) as follows:

$$S = \left(\frac{25400}{CN}\right) - 254 \qquad (3.11)$$

where C.N. is the curve number.

3.10.2. Transform Method

The translation of excess precipitation to runoff is accomplished by using seven methods includes (Clark unit hydrograph, kinematic wave, ModClark, SCS unit hydrograph, Snyder unit hydrograph, user-specified graph, and user-specified unit hydrograph). The SCS unit hydrograph method is used to determine loss, which requires only one parameter for each subbasin “The lag time.” The standard lag is defined as the length of time between the centroid of precipitation mass and the peak discharges of the resulting hydrograph [USGS 2012]. The transform method requires a lag time determination as an input. The SCS developed a relationship between the time of concentration (Tc) and the lag time (Tlag) given by Equation (12). The time of concentration is calculated by Giandotti’s formula given by Equation (13) [GIANDOTTI 1934]. The time of concentration and lag time values will be calculated for 56 subbasins.

$$T\text{lag} = 0.6\,T\text{C} \tag{3.12}$$

$$TC = \frac{4 + \sqrt{H} + 1.5L}{0.8\sqrt{H}} \tag{3.13}$$

Where: Tlag = the lag time; Tc = the time of concentration; A = the watershed area (km2); L = the length of the main channel (km); H = the difference between the mean basin elevation and the outlet elevation (m).

3.11 Parameters Weighting Which Influence Flood Events

To estimate the spatial variability of flood risk in Kyrenia, five different flood Risk Levels (R.L.) were considered (catastrophic, sever, major, minor, and low). Performed classification based on the factors influence to generate flood events. The hazard map was created using the integration of five thematic maps – factors, which includes Flow accumulation (F), Peak discharge (P), Elevation (E), Land use (L), and Slope (S) were created with numeric values using spatial tool analysis in ArcGIS software. The effect of each factor is classified for five Risk Levels (R.L.) as following: catastrophic, sever, major, minor, and low. By applying Jenk's Natural Breaks method for classifications. Furthermore, each of the proposed factors rating of the flood Risk Levels (RL) a numerical value is assigned as follows: catastrophic = 5, sever (RL) = 4, major (RL) = 3, minor (RL) = 2, low (RL) = 1. Considering that all the proposed factors do not have the same degree of influence on flood generation, correlation analysis with different weights for each factor was applied. This analysis considers the effect of each factor on all other factors. Thus, two kinds of effects are employed: (a) major effect, that is, a change of the first factor bears a direct effect on the other [assigned (1) point] and (b) a minor effect, that is, the change of the first factor bears an indirect effect on the other factor [assigned (1/2) point]. The rate for each factor is calculated as the summation of the points of major and minor effects. These rates are presented in Table 3.4. The selection of the factors mentioned above as well as the flood Risk Levels (R.L.) and the Factors Rates (F.R.) were based on the literature and the Delphi approach (Eimers et al., 2000; Yahaya et al., 2010; Kourgialas and Karatzas, 2011; Kazakis et al., 2015). Specifically, according to literature surveys, the five factors mentioned above can capture the necessary information improving the decision-making utility for flood risk modeling (Zerger, 2002).

Table 3.4: Interaction between factors that influence the flood risk [Factors Rates (F.R.)].

Factor Changing	**Major Effect**	**Minor Effect**	**Factor Rate (F.R.)**
Flow accumulation (F)	(L)	(S)	1.5 pts (1major + 1minor)
Slope (S)	(F), (L)		2.0 pts (2major + 0minor)
Land use (L)	(F), (P)	(S)	2.5 pts (2major + 1minor)
Peak Discharge (P)	(F), (E)	(L)	2.5 pts (2major + 1minor)
Elevation (E)	(R), (L), (F)	(S)	3.5 pts (3major + 1minor)

All the factors mentioned above were georeferenced to the Cyprus Coordinate System CGRS93 / Cyprus Local Transverse Mercator (EPSG Projection 6312. Geoinformatics and filed measurement techniques were used to determine and digitalize the aforementioned thematic maps/factors.

CHAPTER 4
RESULTS AND DİSCUSSİONS

4.1 Catchment Area and flow delineation

The catchment area is about 640 km^2, which consists of 56 sub-basins. The geomorphological parameters of the catchment extracted from the QGIS using Saga plug are shown in Table 4.1. The obtained information was used inputs for runoff simulation using the HEC-HMS model to calculate peak discharge and excess of precipitation. Also, to calculate time lag (T_{lag}) and time of concentrations (T_c) based on morphological parameters by applying the SCS method, as summarized in Table 4.2 .

Table 4.1: Geometric and morphological parameters for sub-basins

No.	A (km2)	US Elev.	DS Elev.	L (Km)	H (Ele. Diff)	Slope	X	Y
1	4.89	158.00	2.40	6.29	155.60	2.5%	196093.73	414612.18
2	4.84	126.70	0.60	4.54	126.10	2.8%	196496.02	413037.15
3	18.68	188.80	0.10	7.78	188.70	2.4%	198945.17	411876.82
4	27.87	259.80	0.20	15.78	259.60	1.6%	200911.28	409210.48
5	20.74	206.70	0.20	9.14	206.50	2.3%	198687.26	406687.12
6	12.72	125.70	12.50	7.70	113.20	1.5%	197710.64	404235.39
7	7.90	221.40	39.90	6.17	181.50	2.9%	201725.90	403160.70
8	12.36	253.00	74.50	7.26	178.50	2.5%	204490.63	405153.23
9	19.27	275.80	140.50	9.58	135.30	1.4%	207604.05	405915.80
10	19.65	252.50	160.50	7.74	92.00	1.2%	211002.93	405390.06
11	5.78	833.70	180.70	11.19	653.00	5.8%	206463.06	402581.83
12	13.63	510.00	172.50	8.07	337.50	4.2%	214781.89	406294.84
13	10.42	469.00	188.60	7.35	280.40	3.8%	216244.09	405994.28

Table 4. 1: Continued

No.	A (km2)	US Elev.	DS Elev.	L (Km)	H (Ele. Diff)	Slope	X	Y
14	24.55	833.80	180.60	11.19	653.20	5.8%	219243.80	405858.57
15	12.60	311.80	182.40	6.33	129.40	2.0%	221370.31	403807.05
16	29.69	776.80	183.00	10.66	593.80	5.6%	224165.70	405510.09
17	22.76	610.00	167.00	7.73	443.00	5.7%	228259.91	404466.94
18	15.88	576.00	153.00	10.54	423.00	4.0%	231314.50	403849.22
19	13.95	580.00	148.80	6.45	431.20	6.7%	233385.09	403824.56
20	9.20	555.60	167.00	7.03	388.60	5.5%	235438.11	403467.53
21	7.55	472.00	161.70	5.85	310.30	5.3%	238127.52	404417.62
22	7.01	313.70	167.60	3.13	146.10	4.7%	239594.31	403450.13
23	41.41	561.80	2.00	15.65	559.80	3.6%	208626.42	410248.55
24	7.62	302.40	1.60	3.07	300.80	9.8%	210356.54	411872.04
25	6.14	728.90	4.00	4.94	724.90	14.7%	215969.59	410643.38
26	7.27	519.00	8.00	5.36	511.00	9.5%	217617.46	410601.63
27	8.14	622.00	3.00	5.85	619.00	10.6%	219424.21	410332.45
28	9.19	761.80	3.20	5.85	758.60	13.0%	223548.78	410550.25
29	8.67	674.00	2.70	5.35	671.30	12.5%	224851.76	409841.22
30	11.29	558.80	9.50	4.71	549.30	11.7%	226714.87	409950.92
31	8.44	355.00	0.00	7.73	355.00	4.6%	228692.72	408530.61
32	7.12	451.46	3.60	0.45	447.86	9.0%	231373.36	408799.98
33	6.10	536.80	0.70	6.08	536.10	8.8%	232808.50	408661.91
34	12.27	558.80	6.50	5.54	552.30	10.0%	235671.88	408748.00
35	11.60	578.00	1.80	6.49	576.20	8.9%	237769.67	410898.85
37	3.30	138.80	0.80	2.95	138.00	4.7%	239414.66	409582.30
38	8.73	514.60	0.30	2.95	514.30	6.1%	240812.13	407447.44
39	17.28	493.80	1.00	6.75	492.80	7.3%	243795.01	407881.71
40	14.51	535.00	1.60	7.10	533.40	7.5%	246444.42	408187.44
41	2.83	78.50	0.50	2.73	78.00	2.9%	244314.65	409910.64

Table 4. 1: Continued

No .	A (km2)	US Elev.	DS Elev.	L (Km)	H (Ele. Diff)	Slope	X	Y
42	6.28	343.00	-1.00	4.86	344.00	7.1%	249791.65	409549.56
43	7.48	474.80	2.00	5.55	472.80	8.5%	251076.42	409594.02
44	7.93	503.70	4.00	5.25	499.70	9.5%	252405.71	410372.30
45	7.66	388.00	14.00	4.01	374.00	9.3%	254078.66	411462.48
46	3.76	389.00	5.00	4.00	384.00	9.6%	255955.27	411748.20
47	3.53	248.00	4.00	3.49	244.00	7.0%	259246.52	412511.96
48	4.81	59.00	2.00	1.71	57.00	3.3%	194948.82	416993.17
49	4.22	430.70	8.00	4.03	422.70	10.5%	194812.02	415684.13
50	1.91	45.70	5.00	2.08	40.70	2.0%	195381.90	413781.20
51	3.61	78.80	0.40	2.67	78.40	2.9%	195986.47	410347.48
52	4.71	707.80	170.0	6.60	537.80	8.1%	238127.52	404417.62
53	16.22	647.50	3.60	4.00	643.90	16.1%	212084.90	412841.02
54	7.11	633.00	5.00	5.07	628.00	12.4%	221340.08	410442.62
55	11.59	550.00	1.00	6.66	549.00	8.2%	248214.14	408974.73
56	7.35	263.00	1.00	3.54	262.00	7.4%	256971.01	411970.24

Table 4. 2: Calculated time lag and time of concentrations

Subbsains no.	length of stream(Km)	H (Ele. Diff)	Tc (Hr)	Tlag (Hr)	Tc (Min.)	T_{lag} (Min.)
1	6.29	155.60	1.83	1.10	109.89	65.93
2	4.54	126.10	1.74	1.04	104.26	62.56
3	7.78	188.70	2.64	1.58	158.11	94.87
4	15.78	259.60	3.47	2.08	208.45	125.07
5	9.14	206.50	2.78	1.67	166.62	99.97
6	7.70	113.20	3.03	1.82	181.98	109.19
7	6.17	181.50	1.90	1.14	114.14	68.48

Table 4. 2: Continued

Subbsains no.	length of stream(Km)	H (Ele. Diff)	Tc (Hr)	Tlag (Hr)	Tc (Min.)	T_{lag} (Min.)
8	7.26	178.50	2.33	1.40	140.10	84.06
9	9.58	135.30	3.43	2.06	205.89	123.54
10	7.74	92.00	3.82	2.29	229.39	137.64
11	11.19	653.00	1.29	0.78	77.50	46.50
12	8.07	337.50	1.83	1.10	109.69	65.82
13	7.35	280.40	1.79	1.07	107.21	64.33
14	11.19	653.20	1.52	0.91	90.95	54.57
15	6.33	129.40	2.60	1.56	156.21	93.73
16	10.66	593.80	1.55	0.93	92.94	55.77
17	7.73	443.00	1.53	0.92	91.90	55.14
18	10.54	423.00	1.82	1.09	109.41	65.65
19	6.45	431.20	1.44	0.86	86.26	51.75
20	7.03	388.60	1.57	0.94	94.17	56.50
21	5.85	310.30	1.63	0.98	97.82	58.69
22	3.13	146.10	1.58	0.95	94.87	56.92
23	15.65	559.80	2.60	1.56	155.99	93.59
24	3.07	300.80	1.13	0.68	67.65	40.59
25	4.94	724.90	0.80	0.48	48.25	28.95
26	5.36	511.00	1.04	0.62	62.47	37.48
27	5.85	619.00	1.01	0.61	60.84	36.51
28	5.85	758.60	0.95	0.57	56.92	34.15
29	5.35	671.30	0.96	0.57	57.33	34.40
30	4.71	549.30	1.09	0.66	65.61	39.37
31	7.73	355.00	1.54	0.92	92.40	55.44
32	0.45	#REF!	1.07	0.64	64.38	38.63
33	6.08	536.10	1.03	0.62	61.55	36.93
34	5.54	552.30	1.19	0.71	71.22	42.73

Table 4. 2: Continued

Subbsains no.	length of stream(Km)	H (Ele. Diff)	Tc (Hr)	Tlag (Hr)	Tc (Min.)	T_{lag} (Min.)
35	6.49	576.20	1.22	0.73	72.96	43.78
36	5.79	421.40	1.00	0.60	59.92	35.95
37	2.95	138.00	1.24	0.75	74.59	44.75
38	2.95	514.30	0.90	0.54	53.70	32.22
39	6.75	492.80	1.51	0.90	90.40	54.24
40	7.10	533.40	1.40	0.84	84.06	50.43
41	2.73	78.00	1.53	0.92	91.99	55.19
42	4.86	344.00	1.17	0.70	70.00	42.00
43	5.55	472.80	1.11	0.66	66.47	39.88
44	5.25	499.70	1.07	0.64	64.20	38.52
45	4.01	374.00	1.10	0.66	66.24	39.75
46	4.00	384.00	0.88	0.53	52.66	31.60
47	3.49	244.00	1.02	0.61	61.18	36.71
48	1.71	57.00	1.88	1.13	112.57	67.54
49	4.03	422.70	0.87	0.52	51.99	31.19
50	2.08	40.70	1.69	1.02	101.66	61.00
51	2.67	78.40	1.64	0.98	98.28	58.97
52	6.60	537.80	1.30	0.78	77.95	46.77
53	4.00	643.90	1.09	0.65	65.37	39.22
54	5.07	628.00	0.91	0.55	54.66	32.80
55	6.66	549.00	1.26	0.76	75.54	45.32
56	3.54	262.00	1.25	0.75	74.87	44.92

4.2 Land use -land Cover and Curve Number Estimate

Land use and land cover maps of Kyrenia were extracted using a remote sensing technique for classifying the Landsat-8 rasters with high resolution downloaded from USGS earth explorer. Maximum likelihood classification is employed using NVDI by applying spatial tool analysis using ArcGIS. Land use was classified into five categories, which include vegetation, urban areas, road, pasture, and woods to calculate curve number (CN), as shown in Table 4.3.

Table 4.3: Computed composite SCS-CN for the sub-basins.

Subbasin no.	CN	Subbasin no.	CN	Subbasin no.	CN	Subbasin no.	CN
1	86.64	15	84.50	29	83.38	43	82.62
2	84.10	16	83.78	30	83.70	44	82.90
3	83.68	17	84.00	31	82.90	45	82.90
4	83.90	18	83.78	32	83.00	46	82.80
5	83.52	19	83.88	33	83.00	47	82.90
6	83.00	20	83.52	34	83.10	48	75.08
7	83.00	21	83.70	35	82.52	49	83.00
8	84.50	22	84.40	36	83.16	50	83.50
9	84.80	23	83.78	37	83.80	51	83.10
10	85.10	24	82.90	38	83.00	52	83.70
11	84.20	25	82.80	39	82.90	53	82.90
12	83.50	26	82.90	40	82.80	54	82.90
13	83.72	27	83.00	41	82.80	55	83.00
14	83.88	28	82.86	42	83.20	56	82.90

4.3 Rainfall data analysis:

Daily rainfall (R) data are analyzed statistically. The statistical characteristics including arithmetic mean (Mean) standard deviation (SD), coefficient of variation in percent (CV), minimum (Min.), maximum (Max.), skewness (S) and kurtosis (K), of daily rainfall for the selected region, are summarized in Tables 4.4. Based on the analysis found that the mean values of monthly rainfall are within the range of 0.501-1.624mm. The maximum value of monthly rainfall occurred in December 2001 (02/12/2020) with a value of 40.14mm (see Figure 4.1), and the minimum value of 0mm (see Figure 4.1) was recorded in the summer season for whole years.

Table 4.4: Statistical estimators of the mean monthly rainfall for the period 1995-2016

Year	Mean	SD	CV	Min.	Max.	S	K
1995	0.5840	1.8737	320.83	0.0000	17.0800	5.28	32.69
1996	0.968	2.714	280.31	0.000	30.570	5.65	45.68
1997	0.865	2.412	278.85	0.000	20.360	4.33	22.69
1998	0.836	2.448	292.75	0.000	21.050	4.52	24.23
1999	0.5175	1.6616	321.11	0.0000	18.5300	5.91	46.92
2000	0.946	3.038	321.12	0.000	39.600	7.44	78.48
2001	1.165	3.551	304.73	0.000	40.140	6.16	51.15
2002	0.824	2.421	293.73	0.000	25.620	5.34	38.61
2003	0.970	2.608	269.05	0.000	17.180	3.88	16.17
2004	1.107	3.443	311.07	0.000	24.030	4.13	18.46
2005	0.783	2.472	315.67	0.000	16.090	4.56	21.75
2006	0.787	2.555	324.73	0.000	29.880	6.62	58.43
2007	0.967	3.256	336.84	0.000	32.390	5.70	38.99
2008	0.629	2.404	382.12	0.000	22.370	5.84	39.28
2009	1.460	3.851	263.83	0.000	33.950	4.35	24.61
2010	0.907	3.148	347.05	0.000	30.670	5.55	37.58
2011	1.086	2.793	257.21	0.000	19.440	3.94	17.99
2012	1.624	4.078	251.12	0.000	29.140	3.60	15.28
2013	0.5008	1.2567	250.95	0.0000	8.6400	3.74	16.54

Table 4.4: Continued

Year	Mean	SD	CV	Min.	Max.	S	K
2014	0.974	2.813	288.83	0.000	29.040	5.05	34.48
2015	1.027	2.825	275.01	0.000	27.850	4.85	30.90
2016	0.871	3.073	352.75	0.000	39.430	7.35	74.36
Average	0.9275	0.9730	104.91	0.0005	4.0959	1.16	0.65

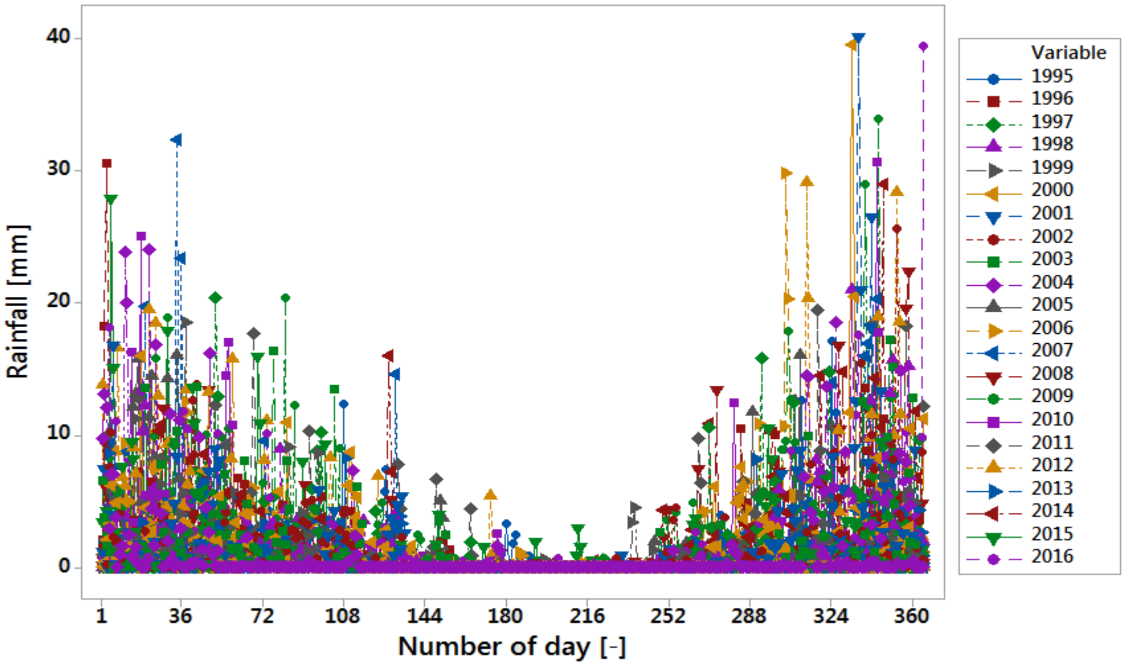

Figure 4.1: Mean daily rainfall during the investigation period (1995-2016)

The distribution parameters were calculated using mean daily rainfall with the maximum likelihood method. The best distribution among the 37-distribution function for the selected location was evaluated based on the Kolmogorov-Smirnov (K-S) test, Anderson-Darling (A-D) test, and Chi-squared (C-s) test. Generally, the distribution with the lowest K-S, A-D, and C-s value will be selected to be the best model for the rainfall distribution in the studied location. The estimated distribution parameters for all selected models are tabulated in Table 4.5. Additionally, Table 4.6 presents the goodness-of-fit statistics for each distribution for average daily rainfall along with a ranking of the distribution models. Based on the K-S test, Beta distribution has the lowest value, which is considered as the best distribution function to study the average daily rainfall characteristics. Based on the A-D and C-s tests, Dagum is among the distribution giving the best fits to investigate the average daily rainfall distribution in the selected regions. Also, it is observed that the inverse Gaussian and inverse Gaussian (3P) distribution functions cannot be used to investigate the average daily rainfall in the studied location based on goodness-of-fit tests, as shown in Table 4.7.

Additionally, based on the A-D tests, Gen. Extreme Value is among the distribution giving the best fits to investigate the maximum monthly rainfall distribution. Moreover, Gen. Gamma (4P) is the best overall model according to the C-s test for the selected location. Also, it is observed that the Exponential, Pareto and Pareto 2 distribution functions cannot be used to investigate the average rainfall in the studied area based on C-s and A-D tests, as shown in Table 4.8 Figures 4.2 and 4.3 illustrate the frequency histograms and probability plots of rainfall of the selected region.

Table 4.5: Distribution parameters for average daily rainfall

Distribution	**Parameters**
Beta	α_1=0.46822 α_2=1.6035 a=0.00136 b=4.5055
Burr	k=3266.6 α=0.71746 β=60883.0
Burr (4P)	k=15.22 α=0.74903 β=26.245 γ=0.00136
Cauchy	σ=0.50084 μ=0.48315
Dagum	k=0.08681 α=5.3135 β=2.7884
Dagum (4P)	k=0.07382 α=6.1753 β=2.9001 γ=0.00136
Exponential	λ=1.079
Exponential (2P)	λ=1.0806 γ=0.00136
Gamma	α=0.89957 β=1.0302
Gamma (3P)	α=0.5358 β=1.8422 γ=0.00136
Gen. Extreme Value	k=0.19758 σ=0.60165 μ=0.43489
Gen. Gamma	k=0.83085 α=0.80478 β=1.0302

Table 4.5: Continued

Distribution	Parameters
Gen. Gamma (4P)	k=2.3112 α=0.2133 β=2.5831 γ=0.00136
Gen. Logistic	k=0.30338 σ=0.44403 μ=0.67919
Gen. Pareto	k=-0.06895 σ=1.1481 μ=-0.14732
Gumbel Max	σ=0.76185 μ=0.487
Gumbel Min	σ=0.76185 μ=1.3665
Inv. Gaussian	λ=0.83368 μ=0.92675
Inv. Gaussian (3P)	λ=0.02834 μ=0.96495 γ=0.00134
Log-Logistic	α=0.87334 β=0.32449
Log-Logistic (3P)	α=0.88776 β=0.41732 γ=0.00136
Log-Pearson 3	α=5.3024 β=-0.83272 γ=3.2969
Logistic	σ=0.53871 μ=0.92675
Lognormal	σ=1.9149 μ=-1.1185
Lognormal (3P)	σ=1.8655 μ=-1.0932 γ=-0.00109
Normal	σ=0.97711 μ=0.92675
Pareto	α=0.18251 β=0.00136
Pareto 2	α=6.7409 β=5.3661
Rayleigh	σ=0.73944
Rayleigh (2P)	σ=1.2787 γ=-0.59582
Wakeby	α=1.1481 β=0.06895 γ=0 δ=0 ξ=-0.14732
Weibull	α=0.64295 β=0.78866
Weibull (3P)	α=0.68697 β=0.73201 γ=0.00136
Erlang	No fit
Erlang (3P)	No fit
Log-Gamma	No fit
Nakagami	No fit

Table 4.6: Distribution parameters for average monthly rainfall

Distribution	**Parameters**
Beta	α_1=1.1705 α_2=0.67678 a=6.7955 b=40.14
Burr	k=259.89 α=3.5531 β=138.54
Burr (4P)	k=202.33 α=3.4093 β=132.3 γ=1.0343
Cauchy	σ=5.692 μ=26.309
Dagum	k=0.29712 α=9.6552 β=33.464
Dagum (4P)	k=179.09 α=33.632 β=242.39 γ=-265.73
Erlang	m=9 β=2.7035
Erlang (3P)	m=85 β=0.89837 γ=-50.28
Exponential	λ=0.03839
Exponential (2P)	λ=0.05745 γ=8.64
Gamma	α=9.6349 β=2.7035
Gamma (3P)	α=85.202 β=0.8982 γ=-50.467
Gen. Extreme Value	k=-0.26593 σ=8.5108 μ=22.952
Gen. Gamma	k=0.98314 α=9.2582 β=2.7035
Gen. Gamma (4P)	k=6.6343 α=0.24738 β=31.177 γ=7.105
Gen. Logistic	k=0.00998 σ=4.8655 μ=25.968
Gen. Pareto	k=-0.96047 σ=28.243 μ=11.641
Gumbel Max	σ=6.5429 μ=22.271
Gumbel Min	σ=6.5429 μ=29.824
Inv. Gaussian	λ=250.97 μ=26.048
Inv. Gaussian (3P)	λ=8.8035E+5 μ=390.15 γ=-364.11
Log-Gamma	α=76.425 β=0.0419
Log-Logistic	α=4.1224 β=24.022

Table 4.6: Continued

Distribution	Parameters
Log-Logistic (3P)	α=74.521 β=359.86 γ=-333.91
Log-Pearson 3	α=4.0197 β=-0.1827 γ=3.9367
Logistic	σ=4.6265 μ=26.048
Lognormal	σ=0.35788 μ=3.2023
Lognormal (3P)	σ=0.04947 μ=5.1144 γ=-140.58
Nakagami	m=2.817 Ω=745.7
Normal	σ=8.3916 μ=26.048
Pareto	α=0.95612 β=8.64
Pareto 2	α=120.7 β=3326.6
Rayleigh	σ=20.783
Rayleigh (2P)	σ=14.51 γ=7.2358
Wakeby	α=96.029 β=11.821 γ=18.49 δ=-0.62737 ξ=7.1962
Weibull	α=2.9935 β=28.629
Weibull (3P)	α=3.3949 β=27.8 γ=1.1004

Table 4.7: Results of goodness-of-fit and ranking of distribution functions based on goodness-of-fit for average daily rainfall for whole years (1995-2016)

Distribution	K-S	Rank	Distribution	D-A	Rank
Beta	0.0637	1	Dagum	1.5748	1
Gen. Gamma (4P)	0.0638	2	Beta	2.3049	2
Dagum	0.0646	3	Weibull	4.8288	3
Dagum (4P)	0.0659	4	Wakeby	5.1802	4
Gamma (3P)	0.0801	5	Gen. Pareto	5.1802	5
Weibull	0.0915	6	Log-Pearson 3	5.3669	6
Log-Pearson 3	0.0957	7	Burr	6.1215	7
Burr	0.099	8	Gen. Gamma	6.2273	8

Table 4.7: Continued

Distribution	K-S	Rank	Distribution	D-A	Rank
Gen. Gamma	0.106	9	Gen. Extreme Value	8.1414	9
Weibull (3P)	0.1105	10	Burr (4P)	8.3949	10
Gen. Extreme Value	0.1135	11	Gumbel Max	9.0348	11
Burr (4P)	0.1152	12	Dagum (4P)	9.4976	12
Log-Logistic (3P)	0.1164	13	Gen. Logistic	9.519	13
Gen. Logistic	0.1213	14	Gen. Gamma (4P)	10.689	14
Wakeby	0.122	15	Gamma (3P)	11.029	15
Gen. Pareto	0.122	16	Lognormal (3P)	12.044	16
Lognormal (3P)	0.1442	17	Lognormal	12.249	17
Lognormal	0.1458	18	Log-Logistic	12.62	18
Gumbel Max	0.1508	19	Weibull (3P)	14.231	19
Logistic	0.1522	20	Normal	16.259	20
Log-Logistic	0.1524	21	Logistic	16.801	21
Gamma	0.1581	22	Gamma	17.649	22
Pareto 2	0.1639	23	Log-Logistic (3P)	18.532	23
Rayleigh (2P)	0.1665	24	Rayleigh (2P)	18.619	24
Normal	0.1718	25	Pareto 2	20.936	25
Exponential	0.1757	26	Cauchy	24.704	26
Exponential (2P)	0.1769	27	Exponential	24.878	27
Gumbel Min	0.1848	28	Exponential (2P)	26.371	28
Cauchy	0.2562	29	Gumbel Min	41.914	29
Inv. Gaussian	0.2688	30	Pareto	74.145	30
Pareto	0.2948	31	Inv. Gaussian (3P)	132.94	31
Rayleigh	0.3047	32	Rayleigh	187.7	32
Inv. Gaussian (3P)	0.4103	33	Inv. Gaussian	381.4	33
Erlang	No fit				
Erlang (3P)	No fit				
Log-Gamma	No fit				
Nakagami	No fit				

Table 4.7: Continued

Distribution	C-s	Rank	Distribution	C-s	Rank
Dagum	11.825	1	Lognormal	86.825	19
Wakeby	17.969	2	Gumbel Min	93.601	20
Gen. Pareto	17.969	3	Gamma	101.59	21
Gumbel Max	24.257	4	Pareto 2	123.16	22
Beta	26.421	5	Exponential (2P)	129.92	23
Normal	36.016	6	Exponential	130.44	24
Gen. Extreme Value	40.182	7	Pareto	166.46	25
Cauchy	46.765	8	Inv. Gaussian	234.83	26
Weibull	48.011	9	Rayleigh	416.76	27
Log-Pearson 3	48.281	10	Inv. Gaussian (3P)	431.46	28
Gen. Logistic	49.347	11	Dagum (4P)	N/A	
Logistic	50.424	12	Gen. Gamma (4P)	N/A	
Gen. Gamma	51.009	13	Gamma (3P)	N/A	
Burr	58.588	14	Weibull (3P)	N/A	
Rayleigh (2P)	60.368	15	Log-Logistic (3P)	N/A	
Burr (4P)	65.656	16			
Log-Logistic	84.155	17			
Lognormal (3P)	85.77	18			

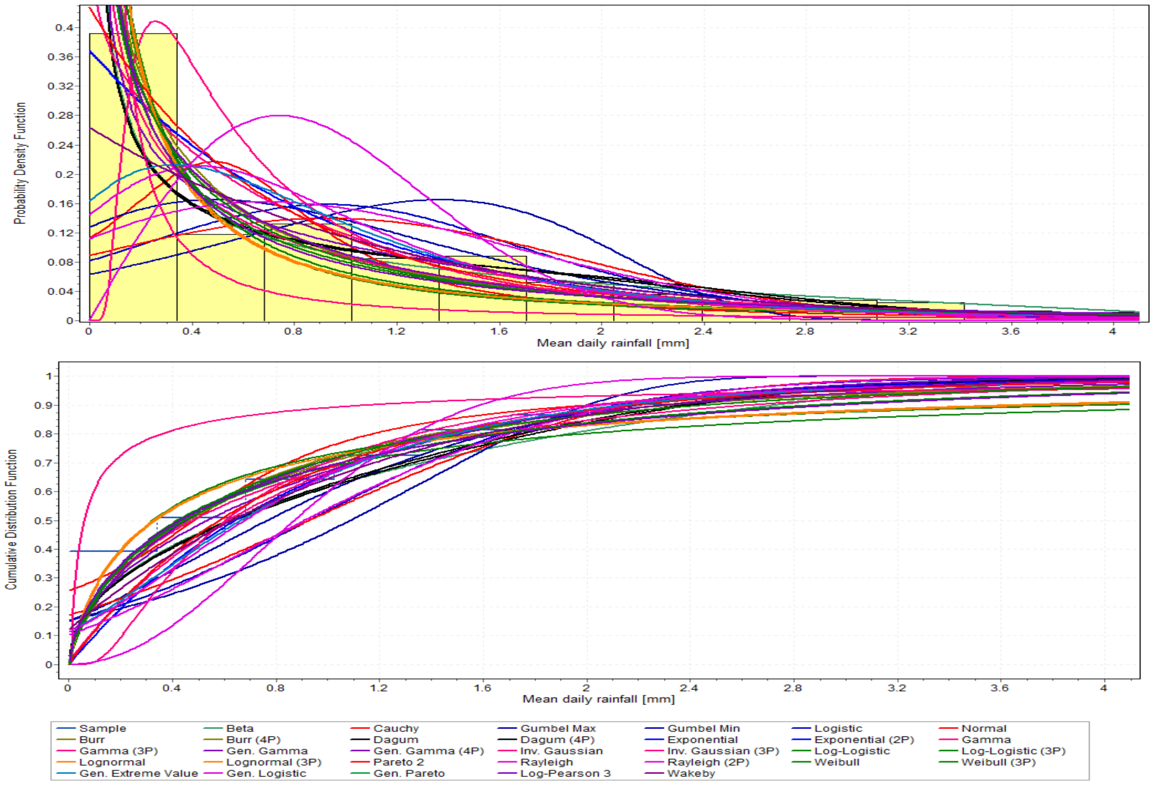

Figure 4.2:Frequency histograms, probability density function and cumulative distribution function plots of average daily rainfall (1995-2016)

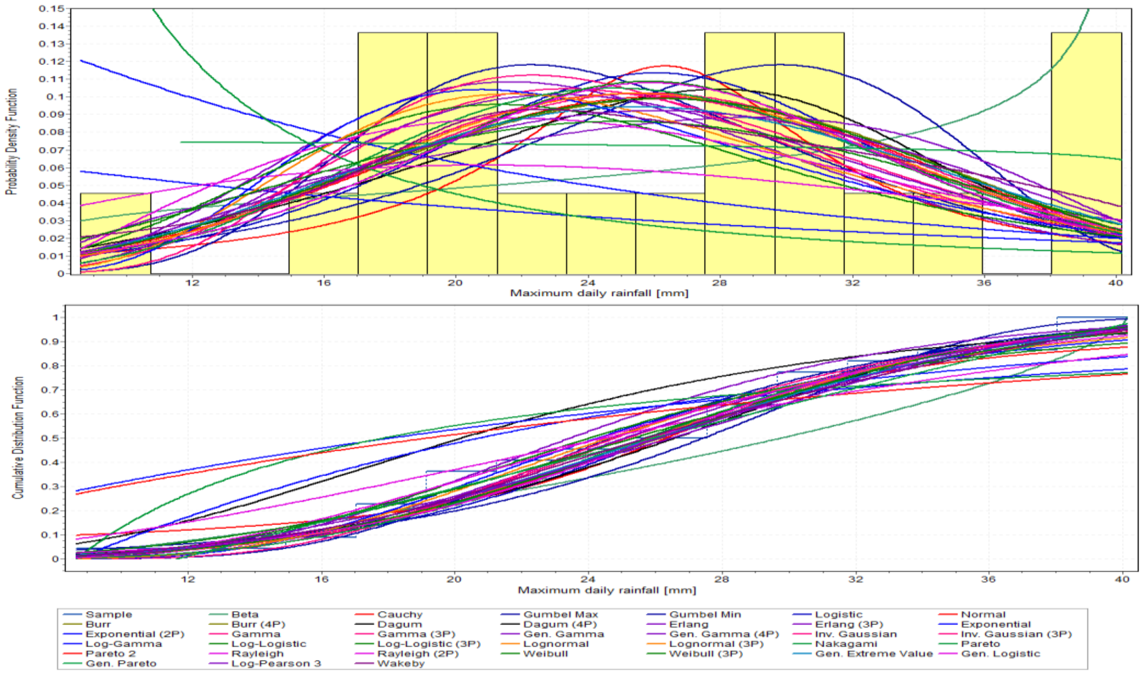

Figure 4.3: Frequency histograms, probability density function and cumulative distribution function plots of maximum daily rainfall

Table 4.8: Results of goodness-of-fit and ranking of distribution functions based on goodness-of-fit for maximum monthly rainfall

Distribution	K-S	Rank	Distribution	A-D	Rank
Log-Pearson 3	0.08139	1	Gen. Extreme Value	0.24113	1
Wakeby	0.08628	2	Wakeby	0.24878	2
Burr	0.08916	3	Log-Pearson 3	0.25351	3
Gen. Extreme Value	0.09073	4	Normal	0.25984	4
Burr (4P)	0.09182	5	Gamma (3P)	0.26344	5
Weibull (3P)	0.09293	6	Erlang (3P)	0.26393	6
Normal	0.09384	7	Lognormal (3P)	0.26732	7
Inv. Gaussian (3P)	0.09685	8	Burr (4P)	0.2688	8
Gen. Gamma (4P)	0.09764	9	Burr	0.26987	9
Dagum	0.10001	10	Weibull (3P)	0.27028	10
Lognormal (3P)	0.10559	11	Inv. Gaussian (3P)	0.27232	11
Erlang (3P)	0.10579	12	Dagum	0.28644	12
Gamma (3P)	0.10657	13	Gen. Logistic	0.28916	13
Gen. Logistic	0.10691	14	Log-Logistic (3P)	0.29459	14
Log-Logistic (3P)	0.10873	15	Nakagami	0.31449	15
Logistic	0.11083	16	Gen. Gamma	0.3184	16
Gen. Pareto	0.11154	17	Gen. Gamma (4P)	0.32974	17
Nakagami	0.1132	18	Weibull	0.33045	18
Weibull	0.11776	19	Gamma	0.33359	19
Cauchy	0.12427	20	Logistic	0.34465	20
Gen. Gamma	0.12651	21	Lognormal	0.41569	21
Gamma	0.12835	22	Inv. Gaussian	0.50485	22
Gumbel Min	0.13521	23	Log-Gamma	0.52673	23
Rayleigh (2P)	0.13546	24	Rayleigh (2P)	0.53371	24
Lognormal	0.13608	25	Gumbel Max	0.55345	25
Log-Gamma	0.14569	26	Log-Logistic	0.58684	26
Inv. Gaussian	0.1459	27	Cauchy	0.58731	27

Table 4.8: Continued

Distribution	K-S	Rank	Distribution	A-D	Rank
Log-Logistic	0.14785	28	Gumbel Min	0.82884	28
Gumbel Max	0.15545	29	Erlang	0.95525	29
Erlang	0.20009	30	Rayleigh	1.3109	30
Rayleigh	0.21349	31	Dagum (4P)	3.2248	31
Beta	0.24349	32	Exponential (2P)	4.0353	32
Dagum (4P)	0.27961	33	Gen. Pareto	4.1422	33
Exponential (2P)	0.30272	34	Pareto 2	4.3803	34
Pareto 2	0.39598	35	Exponential	4.7096	35
Pareto	0.40271	36	Beta	5.1149	36
Exponential	0.41537	37	Pareto	6.4716	37

Table 4.8: Continued

Distribution	C-s	Rank	Distribution	C-s	Rank
Gen. Gamma (4P)	0.03041	1	Burr	1.5301	15
Weibull	0.04906	2	Inv. Gaussian (3P)	1.5326	16
Gen. Gamma	0.12407	3	Weibull (3P)	1.5373	17
Rayleigh (2P)	0.19947	4	Burr (4P)	1.539	18
Log-Logistic	0.24141	5	Lognormal (3P)	1.5431	19
Lognormal	0.25325	6	Gen. Extreme Value	1.5478	20
Log-Gamma	0.26121	7	Gamma (3P)	1.5605	21
Log-Pearson 3	0.3287	8	Erlang (3P)	1.5617	22
Dagum	0.41927	9	Nakagami	1.5916	23
Cauchy	0.57182	10	Gamma	1.6647	24
Wakeby	0.96011	11	Inv. Gaussian	1.7009	25
Gumbel Max	0.98901	12	Rayleigh	2.3482	26
Gumbel Min	1.0279	13	Erlang	2.3805	27
Normal	1.5207	14	Gen. Logistic	2.5472	28

Table 4.8: Continued

Distribution	C-s	Rank	Distribution	C-s	Rank
Logistic	2.5575	29	Dagum (4P)	4.3941	33
Log-Logistic (3P)	2.5597	30	Exponential	7.6221	34
Exponential (2P)	2.9663	31	Pareto 2	7.6547	35
Pareto	3.9732	32	Gen. Pareto	N/A	
			Beta	N/A	

The return period of annual maximum monthly rainfall in the selected region was calculated using a different formula. The rainfall return period is illustrated in Figure 4. 4. The horizontal axis represents the return period in a year, while the vertical axis represents the maximum monthly rainfall. From the analysis, the return period of the 40.14 mm event was within range of 23-44 years, as shown in Figure 4.8. The return period of the 40.14 mm event was 44 years and 23 years according to plotting point applying Hazen and Weibull method, respectively. The estimate of the return periods from the six methods was in agreement. The results indicated that if the design return period of a hydraulic infrastructure being designed is less or equal to the data record period, estimation of quantiles by empirical distribution function or plotting point methods is recommendable.

İn conclusion, the return period of the 40.14 mm event was within range of 23-44 years. The return period of the 40.14 mm event was 44 years and 23 years according to plotting point applying Hazen and Weibull method, respectively. The design rainfall depth was computed by using the Hazen equation, as shown in Table 4.9 .

Table 4.9: Design rainfall for the study area.

Design period	5 Years	10 Years	25 Years	50 Years	100 Years	200 Years
Rainfall	32.46	39.03	47.71	54.28	60.85	67.41

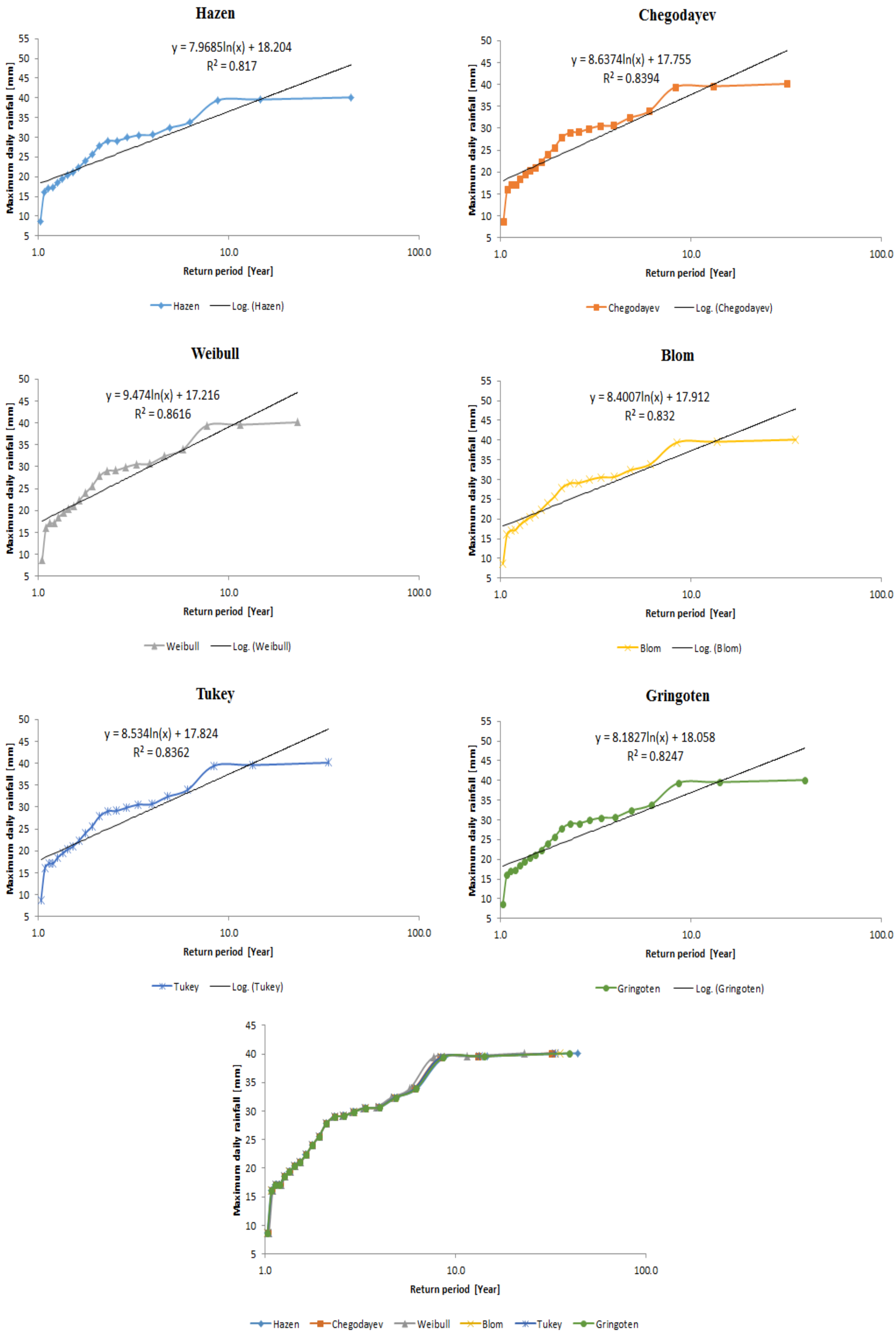

Figure 4. 4: Return period in years computed using six different formulas

4.4 Rainfall-runoff simulation

Synthetic unit hydrograph (SUH) methods were applied since there is no record data for runoff in ungagged catchments. The SCS curve number (SCS-CN) method is used to compute the excess rainfall depth and direct runoff. The HEC-HMS model depends on two significant inputs: sub-basins physical features and the hydrological information. Figures 4.5 and 4.6 present the summary of the computed runoff characteristics, including runoff volume and peak discharge from the HEC-HMS model for different return periods for each subbasin. The excess of precipitation will be used in the hydraulic model.

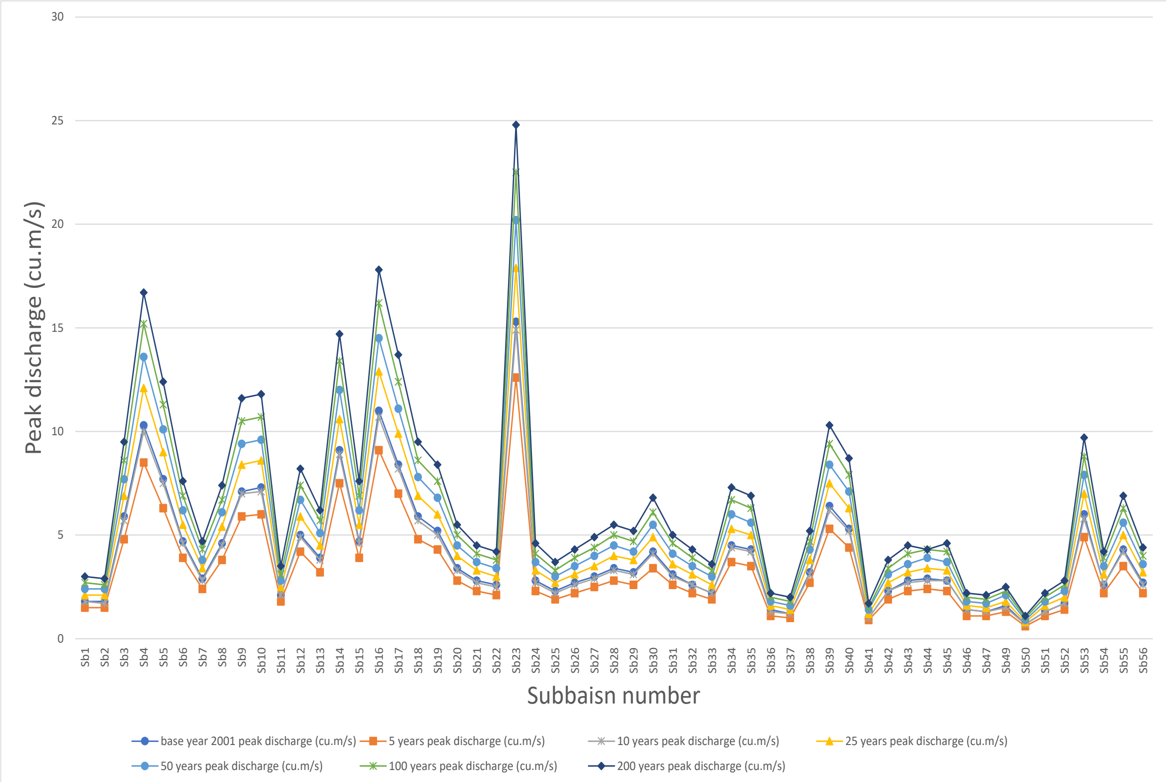

Figure 4.5: Peak discharge based on HEC- HMS simulation

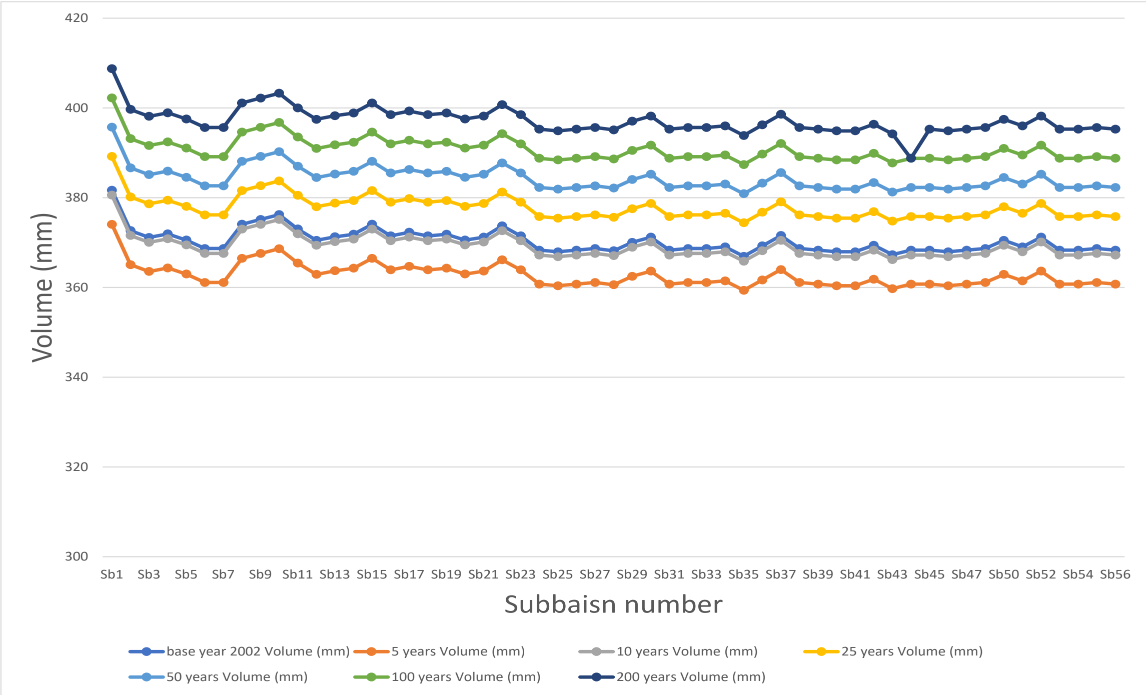

Figure 4.6: Runoff Volume(mm) based on HEC- HMS simulation

4.5 Parameters Weighting and Map Classifications

Five selected factors have the most significant influence on flood risk assessment based on their parameters weightage and rates of factors, considering the cross-pollination between factors. The final percentage of each element regarding its effect on the flood risk occurrence is calculated the total factor weight rate (calculated by multiplied FR and RL) to the overall total weight, as summarised in Table 4.10.

Five thematic maps generated and georeferenced to the Cyprus Coordinate System CGRS93 / Cyprus Local Transverse Mercator (EPSG Projection 6312. Maps reclassified by applying a spatial analysis tool using Arcgis software considering the final percentage for each thematic map factor.

Topographic parameters such as slope and elevation are inversely proportional to the appearance of floods (Kourgialas and Karatzas, 2011); the lowest elevations and slopes can increase flood risk, while higher elevation and slope had minimal influence on flood risk as illustrated in Figures 4.7 and 4.8 and Table 4.10.

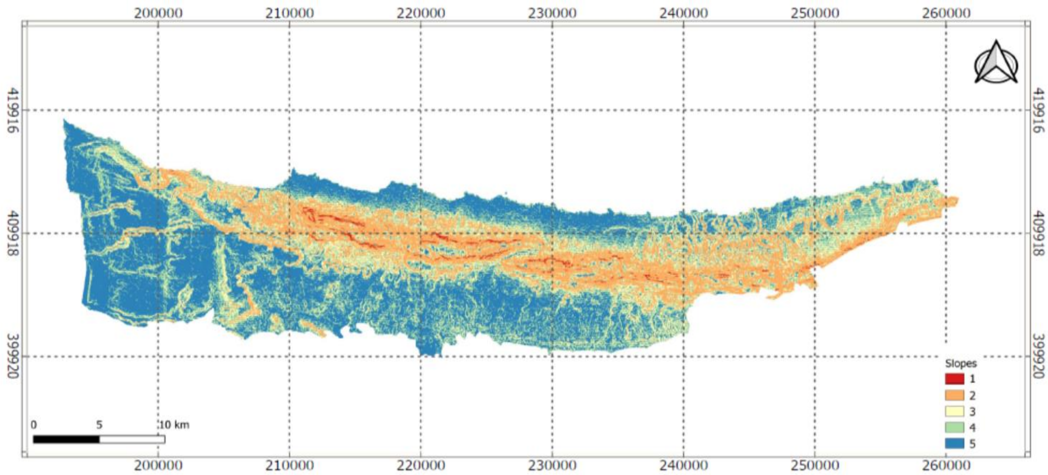

Figure 4.7: Slope thematic map classification

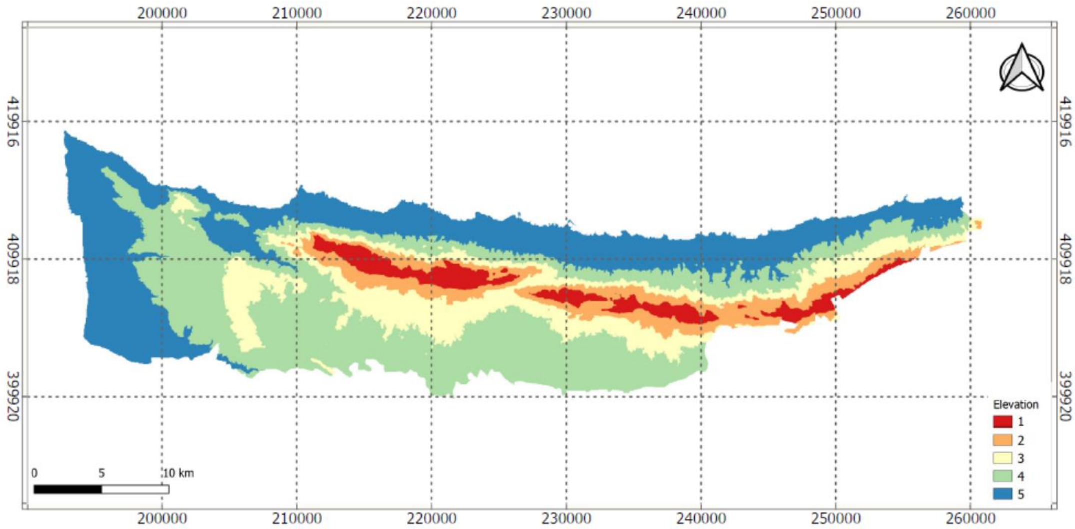

Figure 4.8: Elevation thematic map classification

Also, land sat-8 satellite images used to determine the land use map for Kyrenia. Land use factor is associated directly with the vegetation cover, which controls time for runoff to reach soil surface and amount of precipitation. Thus, dense vegetation in forest and pasture areas can reduce the flood risk, while urban areas without vegetation can lead to increase risk, as illustrated in Table 4.10 and Figure 4.9.

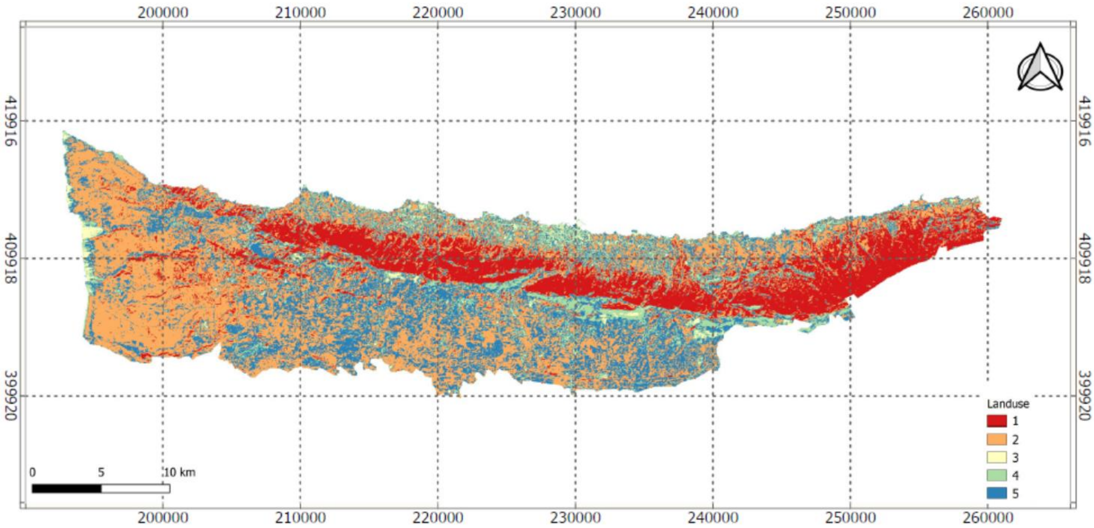

Figure 4.9: Land use thematic map classification

Besides, the flow accumulation map indicates the hydrological contribution for each cell based on the number of pixel cells, where the lower value of the flow accumulation in a pixel-cell is the lower risk level, as illustrated in Table 4.10 and Figure 4.10. Finally, Peak discharge thematic map achieved by applying the Inverse distance weighting (IDW) method, using spatial analysis tools in ArcGIS software. Based on the peak discharge value for each subbasin computed by applying HEC-HMS runoff simulation, as illustrated in Table 4.10 and Figure 4.10.

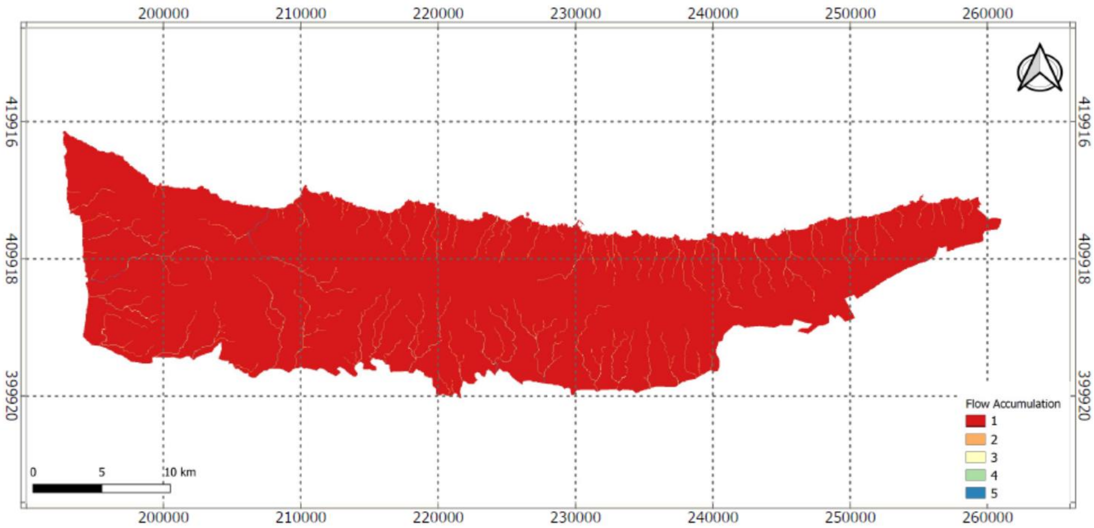

Figure 4. 10: Flow accumulation thematic map classification

Table 4.10: Categorization—calibration and weight evaluation of the factors affecting flood risk areas in Kyrenia

FACTORS	Domain of effect	Descriptive level (flood risk level)	Proposed weight of effect (RL)	Rate (FR)	Weighted rating (FR*RL)	Total weight	Percentage (%)
Slope	0-7.5	Catastrophic	5	2.0	10	30.0	17%
	7.5-15.0	Sever	4		8		
	15.0-25.0	Major	3		6		
	25.0-93.0	Minor	2		4		
	93.0 and above	Low	1		2		
Elevation	-5.0_ 129	Catastrophic	5	3.5	17.5	52.5	29%
	129.0-251.0	Sever	4		14		
	251-398	Major	3		10.5		
	398-603	Minor	2		7		
	603-1020	Low	1		3.5		
Land use (L)	Urban & bare area	Catastrophic	5	2.5	12.5	37.5	20%
	Scrub, annual crops	Sever	4		10		
	Permanent crops	Major	3		7.5		
	Pastures	Minor	2		5		
	Forest-woods	Low	1		2.5		
Flow accumulation (F)	27875 - 52789	Catastrophic	5	1.5	7.5	22.5	13%
	14087 - 27875	Sever	4		6		
	5798 - 14087	Major	3		4.5		
	1525 - 5798	Minor	2		3		
	0 - 1525	Low	1		1.5		

Table 4.10: Continued

FACTORS	Domain of effect	Descriptive level (flood risk level)	Proposed weight of effect (RL)	Rate (FR)	Weighted rating (FR*RL)	Total weight	Percentage (%)
Peak Discharge (P)	8.8 - 15.30	Catastrophic	5	1.5	12.5	37.5	21%
	6.4 - 8.8	Sever	4		10		
	4.5 - 6.4	Major	3		7.5		
	3.0 - 4.5	Minor	2		5		
	0.7 - 3.0	Low	1		2.5		

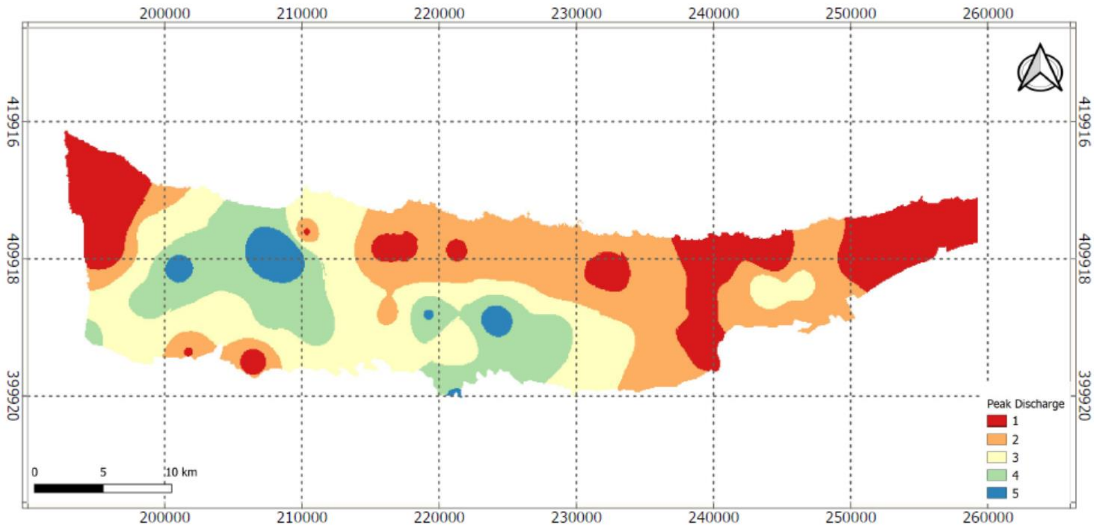

Figure 4.11: Peak discharge thematic map classification

4.6 2D flood mapping and hydraulic model using HEC-RAS

Hydraulic 2D flood mapping was achieved by carrying out unsteady flow conditions using HEC-RAS, based on the excess of precipitation and inflow hydrograph to determine flow depth and water surface elevation for the selected design periods 5,25,50,100 and 200 years. 2D flood mapping for five years estimate the maximum depth of 10 .25 m at downstream and minimum 0.002 m at high elevations area as shown in blue color and classified as the catastrophic degree of risk, as shown in Figure 4.12, for 25 years. Also, 2d flood mapping for design period 25 is showing a bit spread of water around mainstream and channel networks as shown in Figure 4. 13 but in 50 years design period 2d flood map showing more stream spreading as shown in Figure 4.14 .for design periods 100 and 200 years the flood will be significant and dominant as illustrated in Figures 4.15 and 4.16.

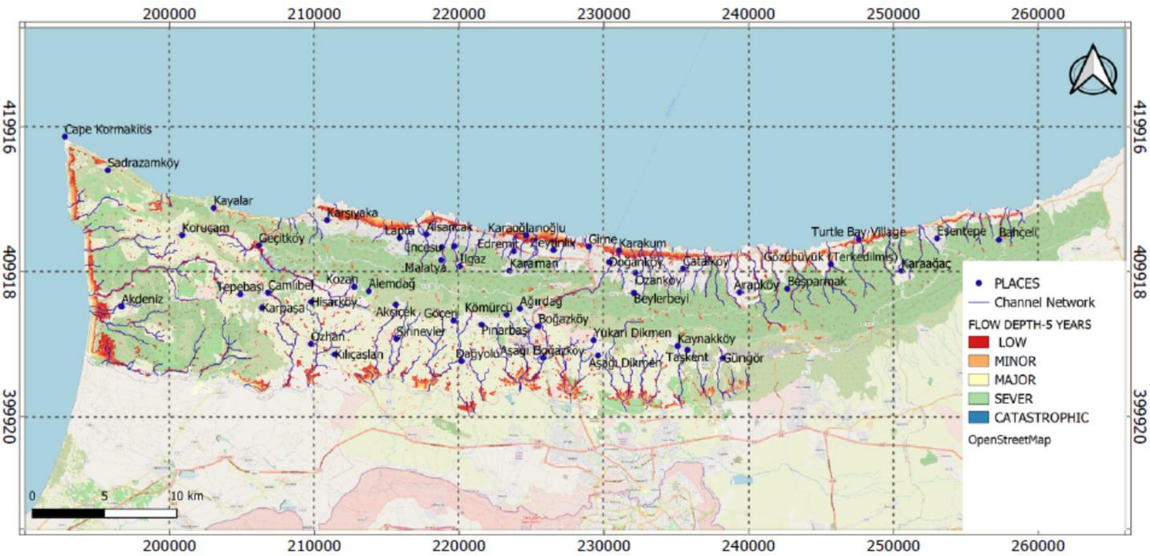

Figure 4.12: Flood inundation map-5 years design period

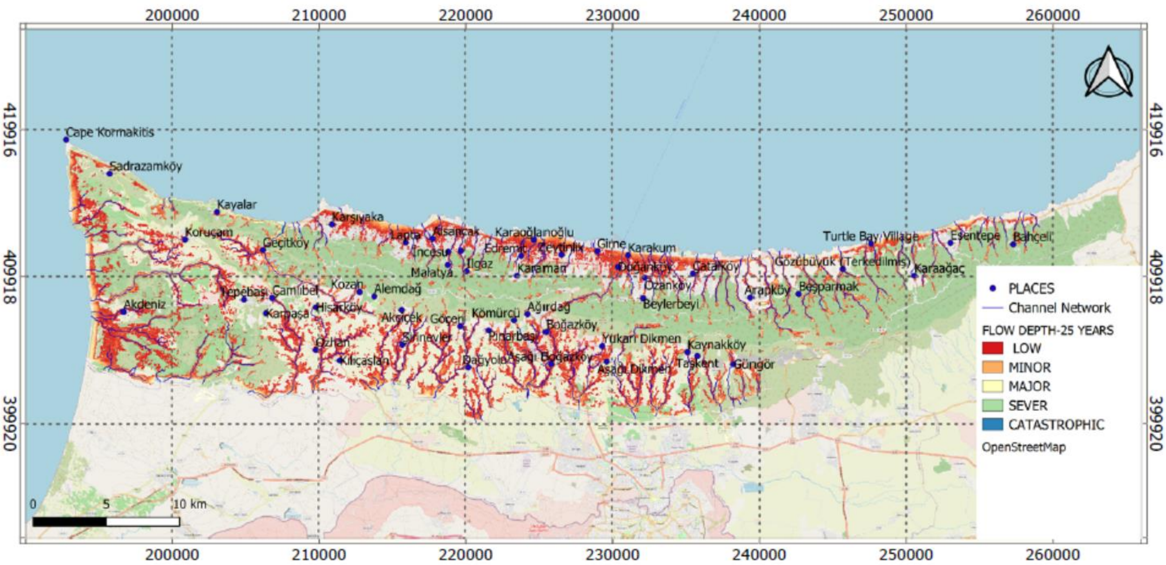

Figure 4.13: Flood inundation map-25 years design period

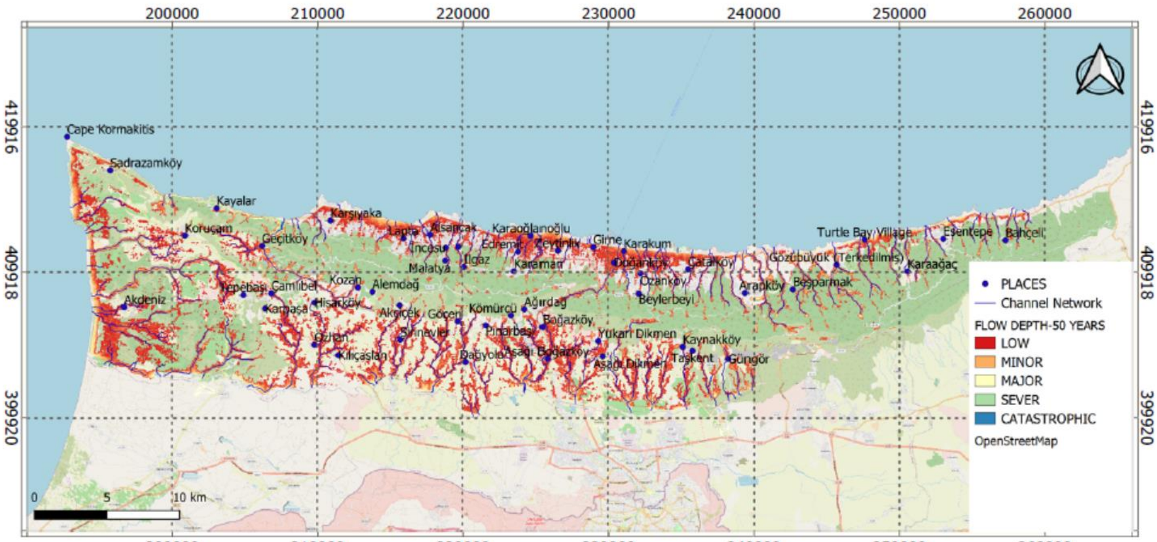

Figure 4.14: Flood inundation map-50 years design period

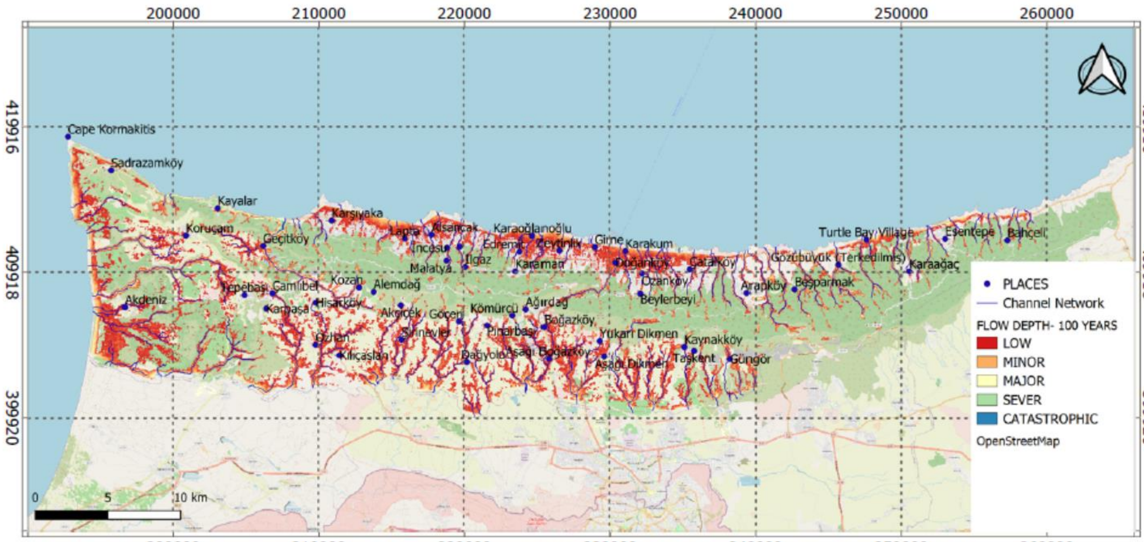

Figure 4.15: Flood inundation map-100 years design period

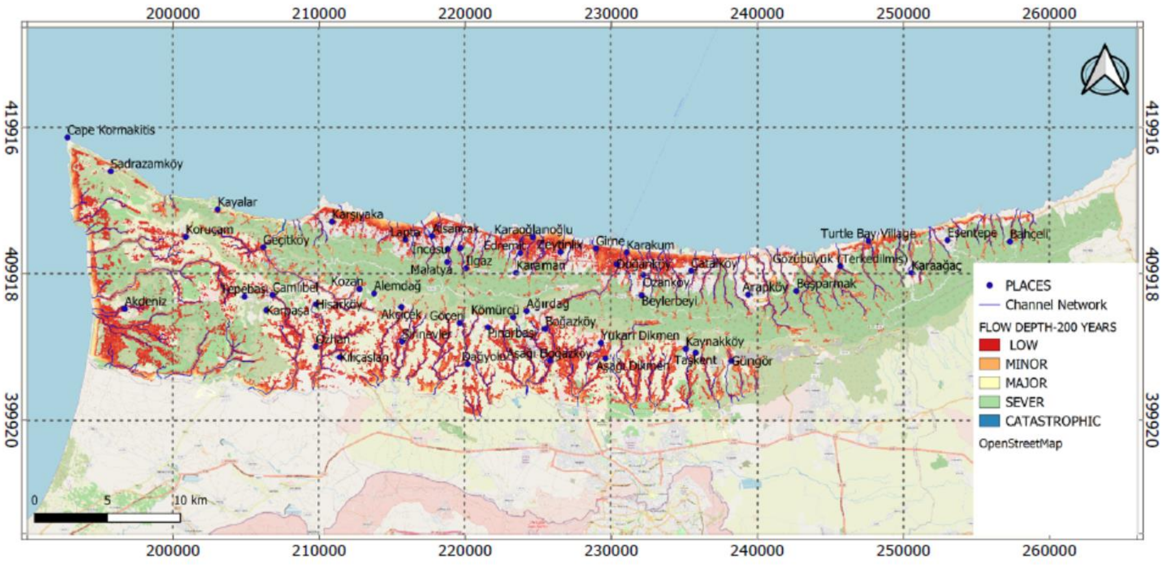

Figure 4.16: Flood inundation map-200 years design period

4.7 Flash Flood Hazard Map

The combination of classified five thematics illustrated in Figures 4.7 to 4.11 includes flow accumulation, slope, elevation, land use, and peak discharge map for different design periods summarized in Table 4.11 are employed to identify prone areas inflicted by flood in Kyrenia. As final results, catastrophic risk areas are distributed in major downstream such as Geçitköy. Also, lowlands are most vulnerable to flood occurrence while the low and minor risk area at the highest land, such as five mountains(Beşparmak), as shown in Figures 4.17 and 4.18.

Table 4.11: Flooded areas for different design periods

RISK LEVEL	Area (m2)				
	5 Years	25 Years	50 Years	100 Years	200 Years
1	30,420,513.00	21,297,995.00	20,069,323.00	17,230,080.00	13,454,050.00
2	162,665,197.00	149,444,828.00	150,160,515.00	130,066,081.00	113,089,402.00
3	455,363,756.00	432,872,113.00	430,204,588.00	353,117,635.00	293,603,257.00
4	18,962,379.00	63,747,579.00	66,921,904.00	166,874,450.00	242,926,740.00

5	6,181.00	55,511.00	61,696.00	129,780.00	4,344,577.00
Total	**667,418,026.00**	**667,418,026.00**	**667,418,026.00**	**667,418,026.00**	**667,418,026.00**
			Percentage of Area		
1	4.56%	3.19%	3.01%	2.58%	2.02%
2	24.37%	22.39%	22.50%	19.49%	16.94%
3	68.23%	64.86%	64.46%	52.91%	43.99%
4	2.84%	9.55%	10.03%	25.00%	36.40%
5	0.00%	0.01%	0.01%	0.02%	0.65%
Total	**100.00%**	**100.00%**	**100.00%**	**100.00%**	**100.00%**

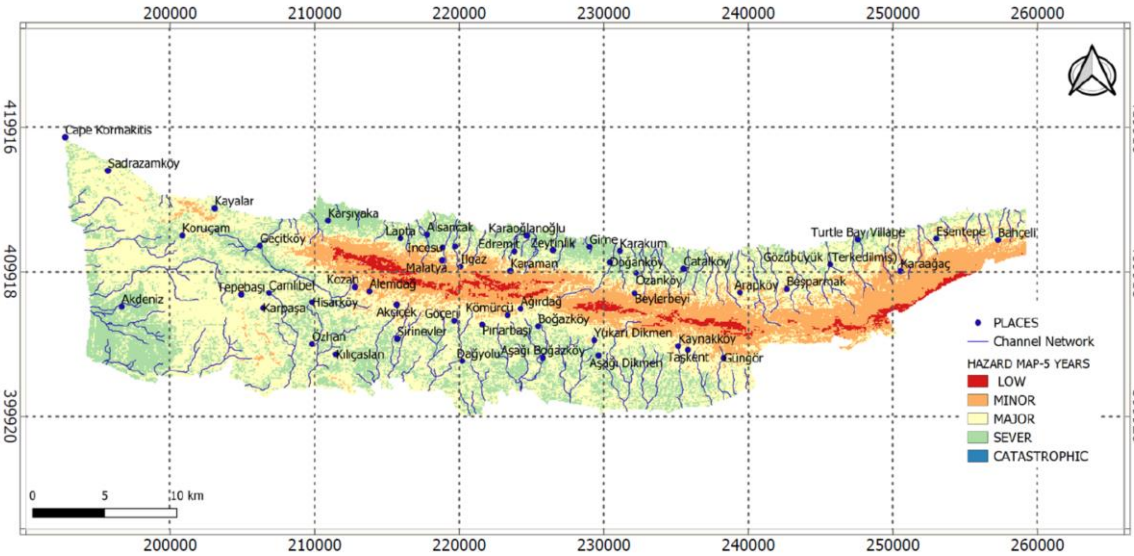

Figure 4.17: Flash flood hazard map-5 years design period

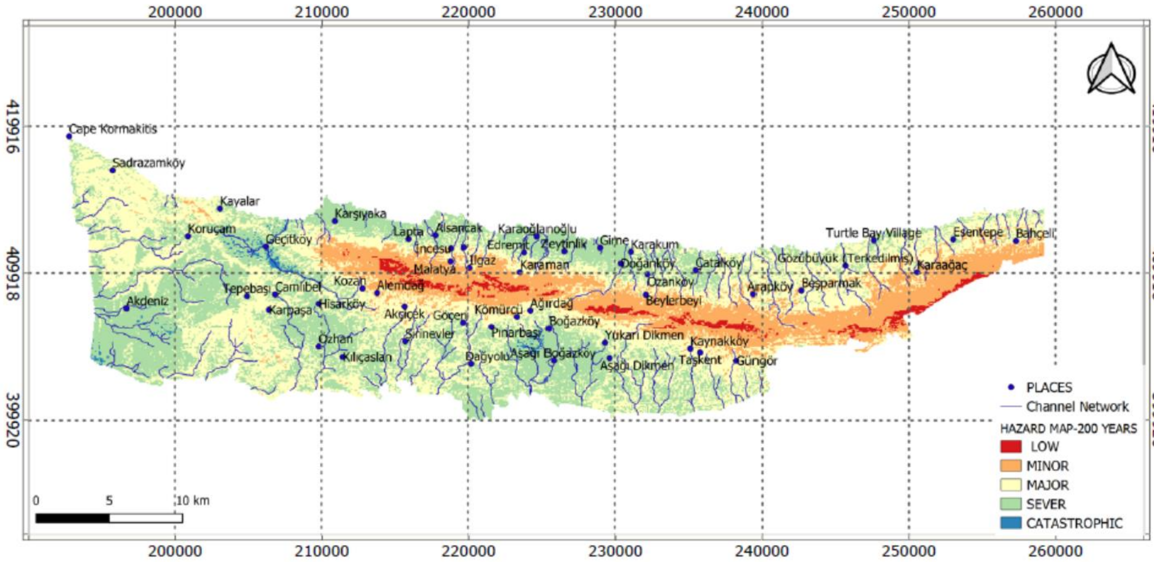

Figure 4. 18: Flash flood hazard map-200 years design period

4.8 Generate a risk flood matrix

The proposed risk matrix is shown in Figure 4.19 based on the impact of flow depth in a horizontal row with classified consequences namely: low, minor, major, severe and catastrophic and the probability of occurrence of return period in vertical row classified to almost certain(every time), likely(1-5 years), possible(25 years), unlikely(25-50 years), rare(100-200 years), which used to define the degree of risk by multiply impact by probability and the results classified into low, medium and high, represented green, yellow and red respectively—quantitative and cost analysis for the risk to be conducted in future works.

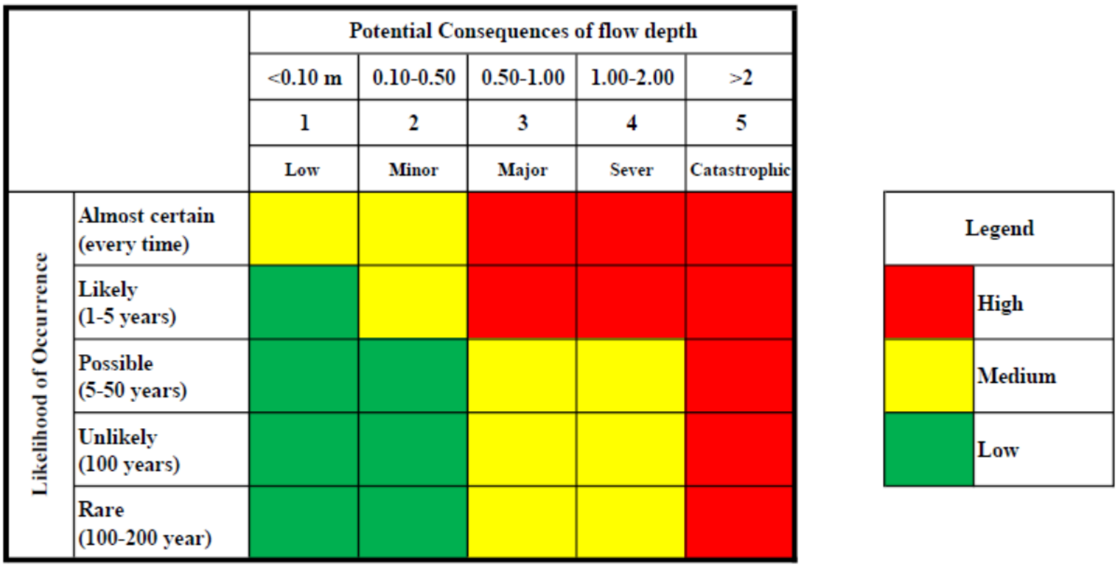

Figure 4.4: Flood risk matrix

4.9 Define Strategies of The Vulnerable Local Communities

Due to the lack of warning system, the response of emergency was weak as reported and discussed in the previous study (Samela,2018) The strategies summarized in Table 4.12 are essential to eliminate risk (Associated,1970).

Table 4. 12: Proposed local communities' strategies

Strategies	Indications for evaluation
Warning system & response	Flood warnings to be increased to reach the most flooded areas. Warning responses to be identified provide evacuation paths. Implement a flash flood warning system based on the France experience using AIGA (method in 2017 (Javelle,2016).

Table 4.12: Continued

Strategies	Indications for evaluation
Response after the flood	Flood insurance, Provide flood assistance plan
Awareness-raising through learning	Warning systems and responses to be learned in schools and companies Internet pages, Accessibility of information for risk map locations.
Mental models analysis	Improving communication and public decision making related to flash flood risk (Lazrus,2016).
Spatial Planning	Flood damage limitation, Natural retention protection for the catchment area. Negative environmental fallout limitation from other flood

4.10 Define Structural Strategies:

The aim of defined structural measures summarized in Table 4.13 to delay the speed of flow and to control flood spread for the non-uniform wadi path cross-sections to reduce the impact of flood culmination.

Table 4.13: Proposed structural strategies

Strategies	Examples and goals
Catchment area and flow path activities	▪ Terraced surrounding land and farms, constructed stone walls. ▪ Small wadi branches bed stabilization. ▪ Add barriers and sandbags ▪ Add dikes
Wadi diversion to redirect floodwater	▪ Depth Control ▪ Slope Control using chutes, concrete lining
Shaping retention to reduce flood	▪ Propose small reservoirs to collect water in a permanent or temporary fashion

CHAPTER 5

CONCLUSION AND RECOMMENDATIONS

5.1 Conclusion

Proposed flash flood mitigation strategies as provided in this study to minimize flood losses human life and constructed structures across Kyrenia, the likeliness of climate change to result in an increase in intense short-duration precipitation in most of Kyrenia and human alterations of the landscape to further increase flash flood risk, being aware of the experiences and lessons learned during a flash flood in Kyrenia area,

5.2 Recommendations

Proposed recommendation are summarized as per the following:

- Generate flooding risk maps to assess planners and decision-makers for the potential impact of floods to avoid.
- A developed web platform data and information to be shared among NMHSs (National Meteorological and Hydrological Services), Authorities, civil defense educational institutions on flash floods awareness.
- Global meteorological data and flash flood guidelines to be provided monitored based on NWP (Numerical Weather Prediction) and nowcasting procedures.
- Local authorities such as water development department to undertake spatial planning considering flash floods hazards.
- The proposed flood risk mitigation plan is illustrated in Figure 5.1.

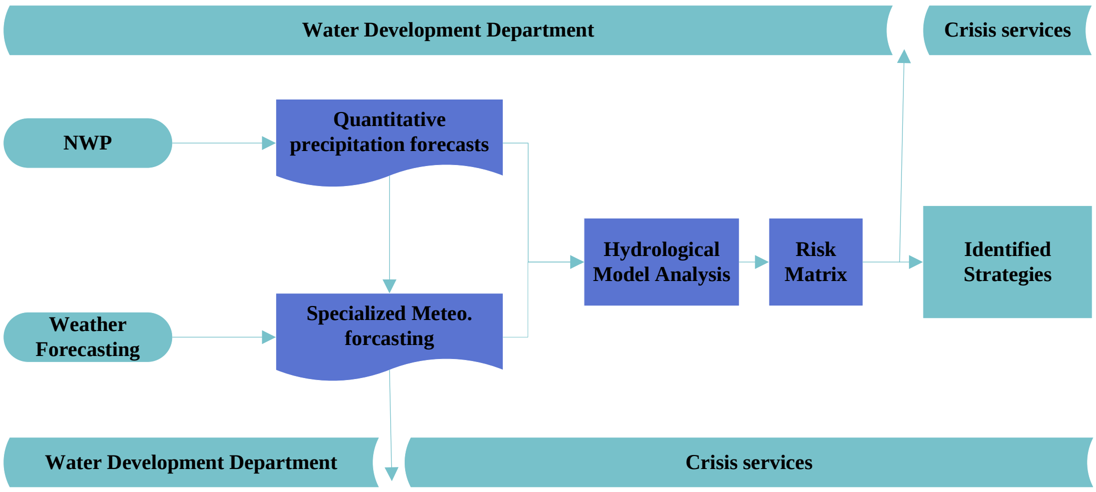

Figure 5.1: Proposed flood risk mitigation plan

REFERENCES

Abuzied, S., Yuan, M., Ibrahim, S., Kaiser, M., & Saleem, T. (2016). Geospatial risk assessment of flash floods in the Nuweiba area, Egypt. *Journal of Arid Environments, 133,* 54–72. https://doi.org/10.1016/j.jaridenv.2016.06.004.

Afshari, S., Tavakoly, A. A., Rajib, M. A., Zheng, X., Follum, M. L., Omranian, E., & Fekete, B. M. (2018). *Comparison of new generation low-complexity flood inundation mapping tools with a hydrodynamic model. Journal of Hydrology, 556,* 539–556. https://doi.org/10.1016/j.jhydrol.2017.11.036.

Agbonaye, A. I., & Izinyon, O. C. (2017). Best-Fit Probability Distribution Model for Rainfall Frequency Analysis of Three Cities in South Eastern Nigeria. Nigerian *Journal of Environmental Sciences and Technology March 2017, 1(1),* 34–42. *doi*: 10.36263/nijest.2017.01.0024.

Aksoy, Hafzullah, S. O. Kirca, Veysel, H. Ibrahim, Kellecioglu, and Dorukhan, n.d., Hydrological and hydraulic models for determination of flood-prone and flood inundation areas: http://adsabs.harvard.edu/abs/2016PIAHS.373..137A.

Alam, M., Farnham, C., & Emura, K. (2018). Best-Fit Probability Models for Maximum Monthly Rainfall in Bangladesh Using Gaussian Mixture Distributions. *Geosciences, 8(4*), 138. doi: 10.3390/geosciences8040138.

Alam, M., Emura, K., Farnham, C., & Yuan, J. (2018). Best-Fit Probability Distributions and Return Periods for Maximum Monthly Rainfall in Bangladesh. *Climate, 6(1),* 9. doi: 10.3390/cli6010009.

Al-Din, S. S. M., Iranfare, M., & Surchi, Z. N. S. (2017). Building Thermal Comfort Based on Envelope Development: *Criteria for selecting right case study in Kyrenia- North Cyprus. Energy Procedia, 115,* 80–91. https://doi.org/10.1016/j.egypro.2017.05.009.

Amin, M. T., Rizwan, M., & Alazba, A. A. (2016). A best-fit probability distribution for the estimation of rainfall in northern regions of Pakistan. *Open Life Sciences, 11(1).* doi: 10.1515/biol-2016-0057.

Arthurton R (1998) Marine-related physical natural hazards affecting coastal megacities of the Asia-Pacific region-awareness and mitigation. *Ocean Coast Manage 40:65–85*.

Associated Programme, 1970, Guidance on Flash Flood Management Recent Experiences from Central and Eastern Europe: http://core.ac.uk/display/22563624.

Baghel, H., Mittal, H., Singh, P., Yadav, K., & Jain, S. (2019). Frequency Analysis of Rainfall Data Using Probability Distribution Models. *International Journal of Current Microbiology and Applied Sciences, 8(06),* 1390–1396. doi: 10.20546/ijcmas.2019.806.168.

Buckland J, Rahman S (1999) Community-based disaster management during the 1997 Red River flood in Canada. *Disasters 23:174–191*.

Cailhol, D., Audra, P., Nehme, C., Nader, F. H., Garašić, M., Heresanu, V., Gucel, S., Charalambidou, I., Satterfield, L., Cheng, H., & Edwards, R. L. (2019). The contribution of condensation-corrosion in the morphological evolution of caves in semi-arid regions: *Preliminary investigations in the kyrenia range, cyprus. Acta Carsologica, 48(1), 5–27*.

CIGLER, B. A. (1996) "Coping with Floods: Lessons from the 1990s" in Disaster Management in the U. S. and Canada, Richard T. Sylves & William L. Waugh, Jr. eds., Charles C Thomas Publisher, Ltd., USA.

CORMEN, T.H., LEISERSON, C.E. and RIVEST, R.L., 1996, Introduction to Algorithms (Cambridge, MA: MIT Press).

Derdour, A., Bouanani, A., & Babahamed, K. (2018). Modeling rainfall-runoff relations using HEC-HMS in a semi-arid region: A case study in Ain Sefra watershed, Ksour Mountains (SW Algeria). *Journal of Water and Land Development, 36(1),* 45–55. https://doi.org/10.2478/jwld-2018-0005.

DECHTER, R. and PEARL, J., 1988, The optimality of A*. In Search in Artificial Intelligence. Kanal and V. Kumar (Eds), pp. 166–199 (New York: Springer).

Divin, J., & Mikita, T. (2016). Effects of land-use changes on the runoff in the landscape based on hydrological simulation in HEC-HMS and HEC-RAS using different elevation data. *Acta Universitatis Agriculturae et Silviculturae Mendelianae Brunensis, 64(3)*, 759–768. https://doi.org/10.11118/actaun201664030759.

Eimers, J.L., Weaver, J.C., Terziotti, S., Midgette, R.W., 2000. Methods of Rating Unsaturated Zone and Watershed Characteristics of Public Water Supplies in North Carolina.

Elfeki A, Masoud M, Niyazi B. 2017. Integrated rainfall-runoff and flood inundation modeling for flash flood risk assessment under data scarcity in arid regions: Wadi Fatimah basin case study, *Saudi Arabia. Nat Haz. 85(1):*87–109.

Elfeki, A., Masoud, M., & Niyazi, B. (2017). Integrated rainfall-runoff and flood inundation modeling for flash flood risk assessment under data scarcity in arid regions: Wadi Fatimah basin case study, *Saudi Arabia. Natural Hazards*, *85(1)*, 87–109. https://doi.org/10.1007/s11069-016-2559-7.

Elfeki, Amro, Mohamed Abdulrazzak, A. E. (23 Jan 2019). Flash flood risk assessment in urban arid environment case study of Taibah and Islamic universities' campuses, Medina, Kingdom of Saudi Arabia. Geomatics, Natural Hazards and Risk.https://doi.org/10.1080/19475705.2018.1545705.

Elkhrachy, I. (2015). Flash Flood Hazard Mapping Using Satellite Images and GIS Tools: A case study of Najran City, Kingdom of Saudi Arabia (KSA). *Egyptian Journal of Remote Sensing and Space Science, 18(2)*, 261–278. https://doi.org/10.1016/j.ejrs.2015.06.007.

ESRI, 2008. ArcView 9.2 User Manuals. Environmental System Research Institute, Redlands, CA. Water-Resources Investigations Reports, Raleigh, NC, pp. 99– 4283.

Exploring facebook affordances in natural disaster: A case ..., 2018:

Farhan, Y., & Ayed, A. (2017). Assessment of Flash-Flood Hazard in Arid Watersheds of Jordan. *Journal of Geographic Information System, 09(06)*, 717–751. https://doi.org/10.4236/jgis.2017.96045.

Faisal IM, Kabir MR, Nishat A (1999) Non-structural flood mitigation measures for Dhaka City. *Urban Water 1*:145–153. doi:10.1016/S1462-0758(00)00004-2.

FEMA (Federal Emergency Management Agency) (2003) Student Manual for Managing Floodplain Development Through *The National Flood Insurance Program (NFIP) Course, Emmitsburg, US.*

Fisher, R., Hobgen, S., Mandaya, I., Kaho, N. R., Timur, T., & Zulkarnain. (2017). Satellite image analysis and Terrain Modelling. 150.

Gaubi I, Chaabani A, Ben Mammou A, Hamza MH. 2016. A GIS-based soil erosion prediction using the revised universal soil loss equation (RUSLE) (Lebna watershed, Cap Bon, Tunisia). *Nat. Hazards, 86(1):*219–239. DOI: 10.1007/s11069-016-2684-3.

Green, J., Xuereb, K., Johnson , F., & Moore, G. (2012). The revised intensity–frequency–duration (IFD) design rainfall estimates for Australia—an overview. Proceeding of 34th Hydrology and Water Resources Symposium 19–22 November 2012, Sydney, Australia.

Hanson, L. S., & Vogel, R. (2008).The Probability Distribution of Daily Rainfall in the United States.*World Environmental and Water Resources Congress 2008*.doi:10.1061/40976(316)585.

Hassan, Z., Shamsudin, S., & Harun, S. (2015). Choosing The Best Fit Distribution For Rainfall Event Characteristics Based On 6H-Ietd Within Peninsular Malaysia. *Jurnal Teknologi, 75(1)*. doi: 10.11113/jt.v75.3058.

Huang, W., Cao, Z., Huang, M., Duan, W., Ni, Y., & Yang, W. (2019). A new flash flood warning scheme based on hydrodynamic modelling. *Water (Switzerland), 11(6)*, 1–15. https://doi.org/10.3390/w11061221.

Javari, M. (2017). Assessment of Temperature and Elevation Controls on Spatial Variability of Rainfall in Iran. *Atmosphere, 8(12)*, 45. doi: 10.3390/atmos8030045.

Javelle, P., D. Organde, J. Demargne, C. Saint-Martin, C. D. Saint-Aubin, L. Garandeau, and B. Janet, 2016, Setting up a French national flash flood warning system for ungauged catchments based on the AIGA method: *E3S Web of Conferences*, v. 7, p. 18010.

Jonkman, S. N., 2005, Global Perspectives on Loss of Human Life Caused by Floods: *Natural Hazards, v. 34*, no. 2, p. 151–175, doi:10.1007/s11069-004-8891-3.

Johnson, F., Haddad, K., Rahman A., Green, J. (2012). Application of Bayesian GLSR to estimate sub-daily rainfall parameters for the IDF revision project, hydrology and water resources symposium, 19–22 Nov 2012. Australia, Sydney.

Kassem, Y., & Gökçekuş, H. (2020). Water resources and rainfall distribution function: a case study in Lebanon. *Desalination and Water Treatment, 177*, 306–321. doi: 10.5004/dwt.2020.24811.

Kara, C., & Akçit, N. (2018). Using GIS for developing sustainable urban growth case Kyrenia region. *International Archives of the Photogrammetry, Remote Sensing and Spatial Information Sciences - ISPRS Archives, 42(3W4)*, 263–268. https://doi.org/10.5194/isprs-archives-XLII-3-W4-263-2018.

Kazakis, N., Kougias, I., Patsialis, T., 2015. Assessment of flood hazard areas at a regional scale using an index-based approach and analytical hierarchy process: application in Rhodope–Evros region Greece. *Sci. Total Environ. 538*, 555–563.

Kourgialas, N.N., Karatzas, G.P., 2011. Flood management and a GIS modelling method to assess flood-hazard areas: a case study. *Hydrol. Sci. J. 56 (2)*, 212–225.

Khudri, M., &Sadia, F. (2013). Determination of the Best Fit Probability Distribution for Annual Extreme Precipitation in Bangladesh. *European Journal of Scientific Research, 103(3)*, 391-404.

King D (2000) You're on our own: community vulnerability and the need for awareness and education for predicTable 2. *natural disasters. J Conting Crisis Manage 8*:223–228.

Kourgialas, N. N., & Karatzas, G. P. (2016). A flood risk decision making approach for Mediterranean tree crops using GIS; climate change effects and flood-tolerant species.

Environmental Science and Policy, 63, 132–142. https://doi.org/10.1016/j.envsci.2016.05.020.

Kourgialas, N.N., Karatzas, G.P., 2011. Flood management and a GIS modelling method to assess flood-hazard areas: a case study. *Hydrol. Sci. J. 56 (2),* 212–225.

Kron W (2002) Keynote lecture: flood risk = flood risk 9 exposure 9 vulnerability. In: Wu B, Huang Z, Wang G, Huang G, Fang H, Huang J (eds) Flood defense 2002: *proceedings of the second international*.

Kundwa, M. J. (2019). Development of Rainfall Intensity Duration Frequency (IDF) Curves for Hydraulic Design Aspect. *Journal of Ecology & Natural Resources, 3(2).* doi: 10.23880/jenr-16000162.

Kwaku, X., & Duke, O. (2007). Characterization and frequency analysis of one day annual maximum and two to five consecutive days maximum rainfall of Accra, Ghana. *ARPN Journal of Engineering and Applied Sciences, 2(5),* 27–31.

Lazrus, H., R. E. Morss, J. L. Demuth, J. K. Lazo, and A. Bostrom, 2016, "Know What to Do If You Encounter a Flash Flood": Mental Models Analysis for Improving Flash Flood Risk Communication and Public Decision Making: https://www.ncbi.nlm.nih.gov/pubmed/26369521.

Lee, C. (2005). Application of rainfall frequency analysis on studying rainfall distribution characteristics of Chia-nan plain in Southern Taiwan. *J Crop Environ Bioinform, 2,* 31–38.

Mamoon, A. A., Joergensen, N. E., Rahman, A., & Qasem, H. (2014). Derivation of new design rainfall in Qatar using L-moment based index frequency approach. *International Journal of Sustainable Built Environment, 3(1),* 111–118. doi: 10.1016/j.ijsbe.2014.07.001.

Mandal, S., & Choudhury, B. U. (2014). Estimation and prediction of maximum daily rainfall at Sagar Island using best fit probability models. *Theoretical and Applied Climatology, 121(1-2), 87–97.* doi: 10.1007/s00704-014-1212-1. Mamoon, A. A., &

Rahman, A. (2016). Selection of the best fit probability distribution in rainfall frequency analysis for Qatar. *Natural Hazards, 86(1),* 281–296. doi: 10.1007/s11069-016-2687-0.

Meena, R. K., Dubey, S., & Basak, S. M. (2019). Use of Different Probability Distribution in Rainfall Analysis for RRS, Pundiari, Cooch Behar. *International Journal of Current Microbiology and Applied Sciences*, *8(10),* 1325–1337. doi: 10.20546/ijcmas.2019.810.155.

MERZ, B. (2004) "Flood risk mapping at the local scale: Concepts and challenges" in Flooding in Europe: Challenges and Development in Flood Risk Management, Advances in Natural and Technological Hazards Research, Kluwer Publishing, Revised Manuscript.

Mitchell J (2003) European river floods in a changing world. Risk Anal 23:567–574.

Michaelides, S., Tymvios, F., &Michaelidou, T. (2009). Spatial and temporal characteristics of the annual rainfall frequency distribution in Cyprus. *Atmospheric Research, 94(4)*, 606-615. doi:10.1016/j.atmosres.2009.04.008.

Montaseri , M., Amirataee , B., & Rezaei, H. (2014). Assessment of Goodness of Fit Methods in Determining the Best Regional Probability Distribution of Rainfall Data. *International Journal of Engineering*, *27(10 (A).* doi: 10.5829/idosi.ije.2014.27.10a.07.

Mohamed, T., & Ibrahim, A. (2016).Fitting Probability Distributions of Annual Rainfall in Sudan. *SUST Journal of Engineering and Computer Sciences, 17(2),* 35-39.

Moser DA. 1997. The use of risk analysis by the U.S. Army Corps of Engineers. Alexandria, VA: *Institute for Water Resources*, *USACE*. p. 34.

Nguyen, H., J. Degener, and M. Kappas, 2015, Flash Flood Prediction by Coupling KINEROS2 and HEC-RAS Models for Tropical Regions of Northern Vietnam: *Hydrology*, v. 2, no. 4, p. 242–265, doi:10.3390/hydrology2040242.

Nharo, T., Makurira, H., & Gumindoga, W. (2019). Mapping floods in the middle Zambezi

Basin using earth observation and hydrological modeling techniques. P*hysics and Chemistry of the Earth, 114(June)*. https://doi.org/10.1016/j.pce.2019.06.002.

Ogunlela, A. (2001). Stochastic Analysis of Rainfall Events in Ilorin, Nigeria. *Journal of Agricultural Research and Development, 1(1)*. doi: 10.4314/jard.v1i1.42189

Okoli, K., Mazzoleni, M., Breinl, K., & Baldassarre, G. D. (2019). A systematic comparison of statistical and hydrological methods for design flood estimation. *Hydrology Research*, *50(6),* 1665–1678. doi: 10.2166/nh.2019.188.

Parchure, A. S., & Gedam, S. K. (2019). Probability distribution analysis of extreme rainfall events in a flood-prone region of Mumbai, India. *Arabian Journal of Geosciences*, *12(11)*. doi: 10.1007/s12517-019-4473-2.

Phien, H. N., & Ajirajah, T. J. (1984). Applications of the log Pearson type-3 distribution in hydrology. *Journal of Hydrology*, *73(3-4),* 359–372. doi: 10.1016/0022-1694(84)90008-8.

PILON, P. J. ed. (2003) "Guidelines for Reducing Flood Losses", United Nations.(http://www.unisdr.org/eng/library/isdr-publication/floodguidelines/ isdr-publication-floods.htm).

Policy for Use of Hydrologic Engineering Center-River Analysis System in the National Flood Insurance Program, n.d.: https://www.fema.gov/policy-use-hydrologic-engineering-center-river-analysis-system-national-flood-insurance-program.

Priess JA, Schweitzer C, Batkhishig O, Koschitzki T, Wurbs D. 2013. Impacts of agricultural land-use dynamics on erosion risks and options for land and water management in Northern Mongolia. *Environ Earth Sci. 73(2):* 697–708. doi:10.1007/s12665-014-3380-9.

Pshenichny, C.A., et al., 2009. The event bush as a semantic-based numerical approach to natural hazard assessment (exemplified by volcanology). *Comput. Geosci. 35 (5),* 1017–1034.

QGIS Project. (2015). QGIS Training Manual. QGIS Project, November, 627.

https://docs.qgis.org/2.8/en/docs/training_manual.

Samela, C., R. Albano, A. Sole, and S. Manfreda, 2018, A GIS tool for cost-effective delineation of flood-prone areas: *Computers, Environment and Urban Systems, v. 70*, p. 43–52, doi: 10.1016/j.compenvurbsys.2018.01.013.

Savage I (1993) An empirical investigation into the effect of psychological perceptions on the Willingnessto- Pay to Reduce risk. *J Risk Uncertain 6:*75–90.

SCHANZE, J. (2006) "Chapter 1: Flood Risk Management – A Basic Framework", pp. 1-20, in Flood Risk Management: Hazard, Vulnerability and Mitigation Measures, Springer.

SCHARFFENBERG W., FLEMING M. 2016. Hydrologic modeling system HEC-HMS v4.2: User's manual. Davis, *USACE, Hydrologic Engineering Center*. pp. 614.

Şen, Z., & Eljadid, A. G. (1999). Rainfall distribution function for Libya and rainfall prediction. *Hydrological Sciences Journal, 44(5),* 665–680. doi: 10.1080/02626669909492266.

SEDGEWICK, R., 2002, Algorithms in C+ +: Part 5 Graph Algorithms, 3rd edition (New York: Addison-Wesley).

Sharma, M., & Singh, J. (2010). Use of probability distribution in rainfall analysis. *N Y Sci J, 3(9)*, 40–49.

Slovic P (1987) Perception of Risk. *Science 236*:280–285.

Sun D, Zhang D, Cheng X (2012) Framework of national non-structural measures for flash flood disaster prevention in China. *Water 4*:272–282. doi:10.3390/w4010272.

Sun D, Zhang D, Cheng X (2012) Framework of national non-structural measures for flash flood disaster prevention in China. *Water* 4:272–282. doi:10.3390/w4010272.

Subyani, A. M., & Al-Amri, N. S. (2015). IDF curves and daily rainfall generation for Al-Madinah city, western Saudi Arabia. *Arabian Journal of Geosciences, 8(12),* 11107–11119. doi: 10.1007/s12517-015-1999-9.

Taha, M. M. N., Elbarbary, S. M., Naguib, D. M., & El-Shamy, I. Z. (2017). Flash flood hazard zonation based on basin morphometry using remote sensing and GIS techniques: A case study of Wadi Qena basin, Eastern Desert, Egypt. *Remote Sensing Applications: Society and Environment, 8(August),* 157–167. https://doi.org/10.1016/j.rsase.2017.08.007.

Tapsell S, Penning-Rowsell E, Turnstall S, Willson T (2002) Vulnerability to flooding: health and social dimensions. *Philos Trans R Soc A 360*:1511–1525.

Tao, D.,Q., Nguyen, V.,T., Bourque, A. (2002). On selection of probability distributions for representing extreme precipitations in Southern Quebec. In: *Annual conference of the Canadian Society for Civil Engineering*, 5–8th June, p 1–8.

Tfwala, C., Rensburg, L. V., Schall, R., Mosia, S., & Dlamini, P. (2017). Precipitation intensity-duration-frequency curves and their uncertainties for Ghaap plateau. *Climate Risk Management, 16,* 1–9. doi: 10.1016/j.crm.2017.04.004.

The human cost of weather-related disasters 1995-2015, n.d.: https://www.unisdr.org/we/inform/publications/46796.

Topics Geo Annual review: Natural catastrophes 2005, n.d.: https://www.preventionweb.net/files/1609_topics2005.pdf.

Tortorelli, R., Asquith, W., & Alan, R. (1999). Depth-duration frequency of precipitation for Oklahoma, US geological survey. *Water Resources Investigation Report, 99*–4232.

United States Department of Agriculture (2007) Hydrologic soil groups. Chapter 7, National Engineering Handbook. (Part 630, Hydrology). *Natural Resources Conservation Service, Conservation Engineering Division, Washington, DC,* p 14.

USUL, N. (1994) Engineering Hydrology, METU-Civil Engineering Department, Ankara.

Van der Veen A, Logtmeijer CJJ (2005) Economic hotspots: visualizing vulnerability to flooding. *Nat Hazards 36(1–2):*65–80.

Wang, L. & H. Liu (2006): An efficient method for identifying and filling surface depressions in digital elevation models for hydrologic analysis and modelling.

International. *Journal of Geographical Information Science, Vol. 20,* No. 2: 193-213.

Y., F., Md., Z., V–T–V., N., S., S., & Y., Z. (2007). Fitting The Best–Fit Distribution For The Hourly Rainfall Amount In The Wilayah Persekutuan. *Jurnal Teknologi*, *46(1).* doi: 10.11113/jt.v46.288.

Yahaya, S., Ahmad, N., Abdalla, R.F., 2010. Multicriteria analysis for flood vulnerable areas in Hadejia-Jama'are river basin Nigeria. *Eur. J. Sci*. Res. 42 (1), 71–83.

Yuan, J., Emura, K., Farnham, C., & Alam, M. A. (2018). Frequency analysis of annual maximum hourly precipitation and determination of best fit probability distribution for regions in Japan. *Urban Climate, 24,* 276–286. doi: 10.1016/j.uclim.2017.07.008.

Zaifoglu, H., Akintug, B., & Yanmaz, A. M. (2018). Regional frequency analysis of precipitation using time series clustering approaches. *Journal of Hydrologic Engineering, 23(6)*. https://doi.org/10.1061/(ASCE)HE.1943-5584.0001659

Zalina, M., Desa, M., Nguyen, V.-T.-A., & Kassim, A. (2002). Selecting a probability distribution for extreme rainfall series in Malaysia. *Water Science and Technology, 45(2),* 63–68. doi: 10.2166/wst.2002.0028.

Zerger, A., 2002. Examining GIS decision utility for natural hazard risk modelling. *Environ. Model. Softw. 17 (3),* 287–294.

Zhang, Y., Wang, Y., Chen, Y., Liang, F., & Liu, H. (2019). Assessment of future flash flood inundations in coastal regions under climate change scenarios—A case study of Hadahe River basin in northeastern China. *Science of the Total Environment, 693*. https://doi.org/10.1016/j.scitotenv.2019.07.356.

APPENDICES

APPENDIX 1

ETHICAL APPROVAL LETTER

YAKIN DOĞU ÜNİVERSİTESİ

ETHICAL APROVAL DOCUMENT

Date: 17/08/2020

To the **Graduate School of Applied Sciences**

The research project titled ''Flash Flood Risk Assessment Based on Historical Measured and Satellite Daily Rainfall Data: Kyrenia Region, Northern Cyprus''has been evaluated. Since the researcher(s) will not collect primary data from humans, animals, plants or earth, this project does not need through the ethics committee.

Near East University ★ Civil and Environmental Engineering Faculty ★

Title:Prof. Dr

Name Surname: Hüseyin Gökçekuş

Signature:

Role in the Research Project: Supervisor

Title: Assist. Prof. Dr.

Name Surname: Youssef Kassem

Signature:

Role in the Research Project: Co-Supervisor

APPENDIX 2

SIMILARITY REPORT

turnitin

Assignments | Students | Grade Book | Libraries | Calendar | Discussion | Preferences

NOW VIEWING: HOME > THESIS > NOUR ATEF ALIJL,FLASH FLOOD RISK ASSESSMENT BASED ON HISTORICAL MEASURED AND SATELLITE DAILY RAINFALL DATA: KYRENIA REGION, NORTHERN CYPRUS

About this page

This is your assignment inbox. To view a paper, select the paper's title. To view a Similarity Report, select the paper's Similarity Report icon in the similarity column. A ghosted icon indicates that the Similarity Report has not yet been generated.

NOUR ATEF ALIJL,FLASH FLOOD RISK ASSESSMENT BASED ...

INBOX | NOW VIEWING: NEW PAPERS ▾

Submit File

Online Grading Report | Edit assignment settings | Email non-submitters

AUTHOR	TITLE	SIMILARITY	GRADE	RESPONSE	FILE	PAPER ID	DATE
Nour Atef Alij	Abstract	0%	--	--		1360034803	20-Jul-2020
Nour Atef Alij	Chapter 4	0%	--	--		1360038016	20-Jul-2020
Nour Atef Alij	chapter 5	0%	--	--		1360038298	20-Jul-2020
Nour Atef Alij	chapter 1	7%	--	--		1360035003	20-Jul-2020
Nour Atef Alij	chapter 2	10%	--	--		1360035336	20-Jul-2020
Nour Atef Alij	chapter 3	10%	--	--		1360036020	20-Jul-2020
Nour Atef Alij	all thesis	15%	--	--		1360030751	20-Jul-2020

Prof. Dr Hüseyin Gökçekuş

Near East University

Environmental Engineering Faculty